Regulation of the pulmonary vasculature by lysophospholipase D autotaxin - lysophosphatidic acid signaling

Hsin-Yuan Cheng

A dissertation submitted to the faculty of the University of North Carolina at Chapel Hill in partial fulfillment of the requirements for the degree of Doctor of Philosophy in the Department of Cell and Molecular Physiology.

Chapel Hill

2009

Approved by: Dr. Susan S. Smyth

Dr. P. Kay Lund

Dr. Kathleen M. Caron

Dr. Beverly H. Koller

Dr. James E. Faber

Abstract

Hsin-Yuan Cheng: Regulation of the pulmonary vasculature by lysophospholipase D autotaxin - lysophosphatidic acid signaling

(Under the direction of Dr. Susan S. Smyth)

Lysophosphatidic acid (LPA) is a bioactive lipid molecule present at physiologically relevant levels in serum that acts by binding to a family of G-protein coupled receptors. Receptor active LPA is produced by the plasma lysophospholipase D enzyme autotaxin/lysoPLD. To define a role for LPA in the pulmonary vasculature, we examined the effect of reduced and elevated circulating LPA in a model of hypoxia-induced pulmonary vasoreactivity. We report that mice carrying one normal and one null allele of the gene encoding autotaxin/lysoPLD (*Enpp2*$^{+/-}$), which have ~ half of plasma LPA, are hyper-reactive to hypoxia-induce vasoconstriction and remodeling as evidenced by the development of higher right ventricular systolic pressures, greater decline in peak flow velocity across the pulmonary valve, and a higher percentage of muscularized arteries at three weeks after exposure to hypoxia. Mice overexpressing human *Enpp2* transgene (Enpp2-Tg) may be moderately protected from hypoxia-induced pulmonary hypertension with less reduction in peak flow velocity across the pulmonary valve after hypoxia

exposure.

Because LPA1 and LPA2 receptors are highly expressed in the cardiovascular system and therefore are candidate receptors to mediate the effects of LPA, we examined the pulmonary vasculature of mice lacking LPA 1 and LPA2 ($LPA1^{-/-}2^{-/-}$). With age, $LPA1^{-/-}2^{-/-}$ mice displayed elevations in right ventricular systolic pressure and developed right ventricular hypertrophy. No differences in pulmonary oxygen saturation, hematocrit, vascular permeability, platelet function, or blood coagulation were observed in $LPA1^{-/-}2^{-/-}$ mice. $LPA1^{-/-}2^{-/-}$ mice had a two-fold decline in peak flow velocity across the pulmonary valve after hypoxia versus wild-type controls, and increased muscularization of the pulmonary arterioles following hypoxia. Taken together, our results suggest that circulating LPA regulates pulmonary vascular pressure by effects on LPA1 and LPA2 receptors.

Acknowledgements

I would like to express my deepest thanks to my advisor, Dr. Susan Smyth, for her constant guidance and encouragement. Her positive attitudes have always motivated me through the hard times of my dissertation work. I am also truly grateful for Susan and all the lab members for creating a fun and pleasant workplace.

The work would not be accomplished without my committee members and collaborators. I thank them for their crucial guidance and countless support.

The collaborative environment at the Department of Cell and Molecular Physiology has really opened me up. Jan McCormick has provided me tremendous help through the years.

My dear friends at Chapel Hill, Ko-Yi, Tsui-Shan, and I-Jen, thank you for exploring the new country with me. Pei-Hsuan and Jui-Hua, thank you for letting me stay at your lovely place every time I came back to Chapel Hill.

I-Fang, Ssu-Yi, Kuei-Ling, Meng-Shuen, Jen-Ruey and Andy, Megan and Bruce, thank you for being my family away from home.

Finally I would like to thank my mom, dad, and brothers for their trust and support from the other side of the world.

Obtaining the PhD degree was not only about the scientific research, but also a journey of life. Thank you all for being part of my journey. I had a great time!

Table of Contents

List of Tables

List of Figures

List of Abbreviations

Ang	angiopoietin
BMP	bone morphogenetic protein
BMPR II	bone morphogenetic protein
cAMP	cyclic adenosine monophosphate
cGMP	cyclic guanosine monophosphate
COX	cyclooxygenase
C_T	threshold cycles
ECE	endothelin-converting enzyme
eNOS	endothelial nitric oxide synthase
Enpp	ectonucleotide pyrophosphatase/phosphodiesterase
ERK	extracellular-signal regulated kinase
ET	endothelin
FS	fractional shortening
H&E	hematoxylin and eosin
LPA	lysophosphatidic acid
LPC	lysophosphatidylcholine
LPP	lipid phosphate phosphatase

LV	left ventricle
LVEDD	left ventricular end-diastolic diameter
LVESD	left ventricular end-systolic diameter
lysoPLD	lysophospholipase D
NO	nitric oxide
PAH	pulmonary arterial hypertension
PAP	pulmonary arterial pressure
PAS-H	periodic acid-Schiff counterstained with hematoxylin
PDE5A	cGMP-specific phosphodiesterase type 5A
PECAM-1	platelet endothelial cell adhesion molecule 1
PlGF	placenta growth factor
PKC	protein kinase C
PPARγ	peroxisome proliferator-activated receptor gamma
PVR	pulmonary vascular resistance
RT-PCR	reverse transcription - polymerase chain reaction
RV	right ventricle
RVSP	right ventricular systolic pressure
S1P	sphingosine 1 phosphate
SMC	smooth muscle cell

TGF-β	transforming growth factor beta
Tie	tyrosine kinase with immunoglobulin-like and EGF-like domains
VEGF	vascular endothelial growth factor
VEGFR	vascular endothelial growth factor receptor
WT	wild-type

Chapter 1

Introduction: Pulmonary development and hypertension

Lung development

The stages of lung development

At around 4-6 week gestation in human and embryonic day 10 (E10) in mice, the development of the lung starts, and continues after birth until completed at ~7 years in human and postnatal day 30 (P30) in mice [1]. Lung development is divided into 4 stages- pseudoglandular, canalicular, saccular, and alveolar stages [1].

The pseudoglandular stage takes place at ~7-16 week gestation in human and ~ E10-16.5 in mice. The development of the lung arises from the laryngotracheal groove, as it forms two parts, the larynx and the trachea. The progenitor cells at the distal part of the primitive trachea give rise to the left and right main-stem bronchi [1,2]. Elongation and branching at the end of the bronchi repeat to form specific lobar, segmental, and lobular branches. The branching process continues into the canalicular stage, which takes place at 16-24 week gestation in human and ~ E16.5-17.5 in mice [3]. All the major lung elements except alveoli are formed, vascularization occurs, and the lumen of the bronchi expands during the

canalicular stage. In the saccular stage, 24-36 week gestation in human and E17.5-P5 in mice, the terminal saccules expand, and the specific respiratory epithelial cells appear, including type I pneumocytes for gas exchange, and type II pneumocytes for pulmonary surfactant secretion. The basal membranes of the type I pneumocytes and the endothelial cells of the capillary contact to form the blood-air barrier to exchange gas [1,2,4]. The final stage is the alveolarization, which occurs after birth (birth to 7 years in human and P5-30 in mice). Alveolarization involves the septation of large primary saccules into smaller air space by the inward protrusion from the wall of the saccules to increase alveolar surface area for efficient gas exchange [3,5].

Alveolarization and angiogenesis tightly associate and coordinate with each other. Capillary vessels flank on one side of the invagitating septae. Later, fusion of the septae and septal capillaries form alveolar walls composed of pneumocytes and endothelial layers to allow gas exchange. The completion of alveolarization requires the spreading of the vasculature [6,7]. Anti-angiogenesis agents prevent alveolarization in rats [8].

Factors affecting lung development include premature birth, hypoxia, early corticosteroid exposure, abnormal regulation/signaling of growth factors (PDGF, FGF, VEGF, TGF-β, and Wnt), and injury of the pulmonary capillaries [1,9,10].

Molecular aspects of alveolarization

Proper microvascular growth is required for alveolarization, and inhibition of angiogenesis results in incomplete alveolarization. Studies have shown the expression levels of angiogenetic markers VEGF/VEGFR2, Ang-1, Ang-2, and Tie-2 are up-regulated, and PlGF/VEGFR1 is at constant level to promote pulmonary microvascular growth during alveolarization in neonatal mouse lung. In the adult mouse lung, PlGF is down-regulated and VEGFR1 is up-regulated to stop angiogenesis, and VEGF/VEGFR2,, Ang-1, Ang-2 and Tie-2 are at relatively high levels for maintenance of the pulmonary microvasculature [11]. Inhibition of angiogenetic molecules often leads to impaired alveolarization. For example, depleting platelet endothelial cell adhesion molecule 1 (PECAM-1) in rats by injecting anti-PECAM-1 antibody after birth results in incomplete alveolar septation in the lung. PECAM-1-null mice also present disruptive pulmonary structure and enlarged alveolar space which is evident as early as P1 [12].

Transforming growth factor beta (TGF-β) is one of the most studied signaling molecules in lung development. TGF-β signals by binding of TGF-β type II receptor, which then recruits and phosphorylates the type I receptor. The phosphorylated type I receptor in turn phosphorylates the downstream receptor-regulated effectors, R-SMADs. The activated R-SMAD binds to the

common-mediator SMAD (co-SMAD) and the SMAD complex translocates to the nucleus to regulate transcription. The most common R-SMADs are SMAD 2 and 3. There are also inhibitory SMADs (I-SMADs) to block the activation of R-SMADs. In general, the TGF-β signaling is anti-proliferative and induces differentiation and apoptosis [1,13].

Compiling evidences have shown that TGF-β is a negative regulator of alveolarization and lung development. Overexpression of TGF-β in the lungs of neonatal mice and rats both leads to impaired alveolar development [14,15]. TGF-β–null mice die either before or shortly after birth with severe inflammation in the hearts and lungs [16]. Neonatal mice expressing a dominant-negative form of TGF-β receptor II are resistant to hypoxia-induced pulmonary vascular remodeling and disruption of alveolarization [17]. Neonatal mice deficient of Thy-1, an inhibitor of TGF-β signaling, show exacerbated responses to hypoxia-induced disruption of alveolar septation. Administration of TGF-β neutralizing antibody to the Thy-$1^{-/-}$ mice is able to rescue the impaired alveolarization [18]. Together, these data suggest that excessive TGF-β signaling has adverse effects on lung development, especially the alveolarization stage.

One the contrary, other studies suggested an alternative relationship between TGF-β signaling and lung development. Mice deficient of SMAD3, one of the

major R-SMAD, display enlarged alveolar space shortly after birth. The disruption of pulmonary structure progresses in an age-dependent manner, as the enlargement of alveoli becomes more evident in older mice [19,20].

One explanation for the dual effects of TGF-β signaling on alveolarization could be that it is dynamically regulated during lung development. In fact, the expression levels of key molecules in the TGF-β signaling pathway are found to vary significantly in mouse lungs throughout the course of lung development [21].

Pulmonary arterial hypertension

Clinical aspects of pulmonary arterial hypertension

The World Health Organization classification of pulmonary hypertension (PH) defines 5 groups: pulmonary arterial hypertension (PAH), PH with left heart disease, PH associated with lung diseases and/or hypoxemia, PH resulting from chronic thrombotic and/or embolic diseases, and miscellaneous PH [22]. PAH, also referred as primary PH, is the focus of this introductory section. The other 4 groups are categorized as the secondary PH.

PAH is characterized by sustained elevation of pulmonary arterial pressure (PAP) and pulmonary vascular resistance (PVR). In humans, PAH is defined by a mean PAP over 25 mmHg at rest or 30 mmHg with exercise, a pulmonary arterial

wedge pressure of 15 mmHg or less, and a PVR of 3 or more Wood units (240 dyn.sec.cm-5) [22,23]. The prevalence of PAH is estimated at ~50,000 to 100,000 in the United States [22,24]. PAH is a progressive and devastating disease with a median survival after diagnosis of 2.8 years [25]. The symptoms of PAH are generally nonspecific, including breathlessness, fatigue, angina, syncope, cough, fluid retention, and exercise-induced nausea and vomiting, and may delay the diagnosis [26]. Treatments of PAH include lifestyle modifications, conventional treatments, such as diuretics, oxygen supplementation, anticoagulation agents, and disease-specific treatments, which will be discussed in more detail below [27]. Yet, the efficacy of current treatments remains unsatisfied with relatively small groups of patients responding effectively to the treatments [28-30].

Molecular aspects of pulmonary arterial hypertension

The pulmonary circulation is highly-compliant with high blood flow, low pressure, and low resistance to adapt large changes in blood flow with little alteration of pressure. In particular, contraction of pulmonary vascular SMCs is tightly regulated by a balance between vasodilators and vasoconstrictors. When the balance fails, pulmonary vascular resistance and arterial pressure elevate, and PAH ensues with remodeling of the pulmonary arteries [22,27,29]. The pulmonary

endothelial cells are the major contributors for the vasodilators and vasoconstrictors, and therefore endothelial cell dysfunction which leads to inadequate secretion of these factors may be an initial cause of PAH [29,31]. Three major vasoconstricting and vadodilatory pathways in the pulmonary vasculature are the nitric oxide, endothelin, and prostacyclin pathways, which are discussed in more detail below.

Nitric Oxide

In the pulmonary vasculature, nitric oxide (NO) is a potent vasodilator produced by endothelial NO synthase (eNOS) from $_{L}$-arginine in vascular endothelial cells. The released NO targets vascular SMCs to stimulate cyclic GMP (cGMP) production, which decreases cytosolic calcium levels and promotes muscular relaxation. The termination of NO signaling occurs by hydrolysis of cGMP by the cGMP specific phosphodiesterase type 5A (PDE5A) [27]. NO also acts on endothelial cells to inhibit the production of endothelin, a vasoconstrictive factor [27].

eNOS is expressed predominantly in the vascular endothelial cells, as well as airway epithelium and certain other cell types, and is the major contributor for NO synthesis in the pulmonary circulation [32,33]. Previous studies reveal a strong link between eNOS activity and the development of hypertension. A reduction in eNOS

expression is found in the lungs of primary PAH patients. Pulmonary vascular endothelial cells from severe cases showed little or no eNOS expression when compared to those from normal subjects [34]. Mice genetically deficient of eNOS develop systemic hypertension [35], while mice overexpressing eNOS display systemic hypotension [36]. eNOS$^{-/-}$ mice are hyperresponsive to hypoxia and develop exaggerated elevations in right ventricular systolic pressure and have a higher incidence to develop right ventricular hypertrophy [37,38]. On the other hand, mice overexpressing eNOS are protected from hypoxia-induced PAH [36]. Mild hypoxia exposure of neonatal eNOS$^{-/-}$ mice results in disrupted alveolarization and reduced vessel density in the lung. VEGRFII expression is lowered in hypoxic eNOS$^{-/-}$ mice, suggesting the NO signaling is required in normal lung septation through preservation of VEGFRII signaling [39]. Therefore certain common mediators, such as eNOS, are required for regulation of pulmonary pressure and development.

Multiple mechanisms have been shown to regulate eNOS activity. Various hormones and cytokines such as estradiol and VEGF stimulate eNOS intracellular translocation by elevating cytosolic calcium concentrations. Shear stress and isometric vessel contraction also modulate eNOS activity via phosphorylation of diverse G protein-coupled receptors [40,41].

Therapies that target the NO pathway in the PAH includes NO or nitrate donor supplements, PDE5A inhibition, and calcium channel blockade [23,27,29].

Prostacyclin

Prostacyclin is produced from arachidonic acid by cyclooxygenases (COX) and prostacyclin synthase in endothelial cells. COX-2 and prostacyclin synthase are thought to be the two major enzymes for prostacyclin production [27,42]. On the other hand, COX-1 is responsible for producing thromboxane A2, a vasoconstrictor [42]. Selective blockage of COX-2 leads to an imbalance between prostacyclin and thromboxane A2 [43,44]. Upon secretion and subsequent uptake by the prostacyclin receptor on SMCs, prostacyclin induces vasodilation by stimulating cyclic AMP (cAMP) production to trigger cAMP-PKA- dependent SMC relaxation [27,29].

Mice deficient of COX-2 show exacerbated PAH comparing to WT controls in the setting of hypobaric-hypoxia [45]. Prostacyclin receptor knockout mice also show similar responses to hypobaric-hypoxia- induced PAH [46]. Prostacyclin levels and prostacyclin synthase activity are reduced in PAH patients [47]. Clinically, intravenous injection or inhalation of prostacyclin and its analogous have been used to treat PAH [27,29].

Endothelin

Endothelin (ET), produced predominantly by endothelin-converting enzymes (ECE) in the endothelial cells, is a 21-amino acid peptide. Three isoforms of ETs have been identified, ET-1, ET-2, and ET-3. ET-1 is the major isoform which, upon secretion, acts on neighboring SMCs in a paracrine manner to induce SMC constriction and proliferation [27]. The receptors for ET are G-protein couple receptors, ET_A and ET_B. ET_A is expressed predominantly in SMCs, and ET_B expresses in both SMCs and endothelial cells. Both ET_A and ET_B mediate vasoconstriction and proliferation of the SMCs. However, the endothelial ET_B serves as a vasodilatory receptor to stimulate the release of NO and prostacyclin, two vasodilators. Endothelial ET_B is also responsible for uptake and hence clearance of ET [27,29]. ET release is regulated by gene expression and peptide synthesis because endothelial cells do not store it. The most potent factor to regulate the synthesis of ET is blood flow. Increases in blood flow trigger vasodilation by activating shear stress receptors on endothelial cells to produce and secrete NO and prostacyclin. These vasodilators in turn inhibit ECE and ET synthesis [27,48].

Acting as the most potent vasoconstrictors in the pulmonary vasculature, ET expression is found to be up-regulated in the lung of PAH patients [49]. Plasma ET-1 levels correlate with the severity of PAH [50,51]. Knockout and transgenic animal

models have revealed roles for the ET pathway in embryonic development, but not much information is available on the development of PAH [52,53]. For example, ET-$1^{-/-}$ mice die of respiratory failure likely due to mechanical obstruction of craniofacial abnormalities at birth. ET-$1^{+/-}$ mice show mild but significant elevation of systemic blood pressure [54]. ET-1 transgenic mice display fibrosis in multiple tissues including lung and kidney, but otherwise normal right ventricular systolic pressures [55,56]. Interestingly, Han *et al.* reported in an abstract that knocking out ET-2, a less studied endothelin isoform, results in impaired alveolarization and RV hypertrophy in mice [151]. Treatments of PAH targeting the ET pathway are endothelin receptor antagonists, such as the dual (ET_A and ET_B) receptor antagonist bosentan, and selective ET_A antagonists sitaxsentan and ambrisentan. [29].

Bone morphogenetic protein

In the classic view of PAH, SMCs contract and proliferate in response to the sustained imbalance of vasoconstrictors/vasodilators secreted form endothelial cells. However, compiling evidences indicate SMC dysfunction could also be a direct cause of PAH. One example is the bone morphogenetic protein (BMP) pathway. BMP is a negative regulator of SMC growth. Loss-of-function mutations of BMP receptor II (BMPRII) are found in high incidences in PAH patients

(50-60% of familial PAH patients, and 10-20% of idiopathic PAH patients) [23,57-59]. Although the loss of BMPRII signaling could induce endothelial apoptosis and lead to PAH [60], studies have shown that it also results in proliferation of cultured pulmonary arterial SMCs [57,61]. PPARγ is thought to be the downstream effector to mediate the anti-proliferative response of BMP in the SMCs, and deletion of PPARγ in mice leads to PAH with increased right ventricular systolic pressure (RVSP), RV hypertrophy, and pulmonary vascular remodeling [57].

Chapter 2

Introduction: Autotoxin/LysoPLD and LPA signaling

Lysophosphatidic acid

Lysophospholipids are derivatives of glycero- and sphingophospholipids lacking one O-acyl chain. Lysophosphatidic acid (1-acyl 2-hydroxyl glycerol 3-phosphate, LPA) and sphingosine-1-phosphate (S1P) are two major bioactive lysophospholipids with wide-ranging biological effects including cell proliferation, apoptosis, adhesion., migration, and invasion [62]. LPA circulates in blood, and is bound to plasma proteins, such as albumin, and found in lipoprotein particles. Most of the effects of LPA are mediated by binding to G-protein coupled receptors, which will be discussed in detail below.

The production and degradation of LPA

Physiological relevant levels of LPA can be detected in the blood. LPA is present in human plasma at ~ 0.1 μM, and are ~ 10-fold higher in serum [63]. The steady state of circulating LPA is balanced between opposing pathways of LPA

synthesis and degradation. A variety of pathways are proposed to be participated in *de novo* synthesis or through phospholipase-catalyzed hydrolysis of phospholipids to produce LPA. However, the primary route of circulating LPA production involves hydrolysis of lysophosphatidylcholine (LPC) by the secreted enzyme autotaxin/lysophospholipase D (lysoPLD) [64]. Autotaxin/lysoPLD is a member of the ectonucleotide pyrophosphatase/phosphodiesterase (Enpp) family, designated Enpp2, with a unique ability to hydrolyze LPC.

Homozygous deletion of *Enpp2* in mice results in embryonic lethality. $Enpp2^{-/-}$ mice die approximately around E9.5~E10.5 due to vascular defects in yolk sac and embryo, and failure of vessel maturation [65,66]. Heterozygous *Enpp2* mice ($Enpp2^{+/-}$) are viable without showing obvious developmental defect and have approximately half of normal circulating autotoxin/lysoPLD and LPA levels. Our group recently found that $Enpp2^{+/-}$ mice were prone to thrombosis [63]. On the contrary, mice transgenically overexpressing autotaxin/lysoPLD (Enpp2-Tg) with elevated circulating LPA level, have bleeding diathesis and attenuated thrombus formation. Exogenous administration of LPA elevates circulating LPA level and recapitulates the bleeding phenotype of Enpp2-Tg mice. The phenotypes could be due to accumulation of autotaxin/lysoPLD in aggregated platelets and platelet-rich thrombus, and binding to activated platelets in a β3 integrin-dependent manner [63].

Inactivation of LPA in the circulation likely involves activities of the lipid phosphate phosphatase (LPP) family of cell surface integral membrane proteins [67]. LPP activity, protein and mRNA can be detected in various cell types including platelets, leukocytes, vascular endothelial cells and SMCs [68,69]. Inactivation of LPP2, one of the three mammalian LPP genes in mice, has been reported to produce no phenotype although circulating LPA levels have not been measured in these animals [70]. A recent report also states no remarkable phenotypes when inactivating LPP1 in mice [71]. By contrast, inactivation of the LPP3 gene results in early embryonic lethality but LPP3 heterozygotes are viable [72]. The production, degradation, and signaling of LPA is illustrated in **figure 2.1**.

Signaling of LPA

LPA acts through binding to a family of G protein-coupled receptors (GPCRs). To date, there are at least five bona fide LPA receptors, LPA1-5 [62,73], with at least three more potential ones (LPA 6 – 8)[74,75]. Evidences also show that LPA may serve as an endogenous activator of PPARγ [76,77]. LPA1-3 belong to the original Edg class receptors, whereas most of the more recently identified LPA receptors show greater sequence identity with purinergic receptors. LPA receptors 1 – 5 are expressed ubiquitously in most mammalian tissues. Bound to circulating LPA, these LPA

receptors couple to multiple heterotrimeric G proteins ($G_{i/o}$, $G_{q/11/14}$, G_s, and $G_{12/13}$) and initiate various signal transduction pathways [78]. **Figure 2.2** shows a schematic network of LPA signaling through receptors, G proteins, and downstream effectors. *In vitro* studies in cell lines reveal that LPA receptors share certain function redundancy as well as specificity [62,79,80]. Several LPA receptors deleted mice were reported. $LPA1^{-/-}$ mice show craniofacial dysmorphism, reduced size, a small incidence of perinatal frontal hematoma, increased apoptosis in sciatic nerve Schwann cells, and 50% neonatal lethality [81]. Deletion of Lpa3 results in implantation defects [82,83]. $LPA3^{-/-}$ female mice produced significantly reduced litter size due to delayed implantation and altered embryo spacing [83]. Lpa2-deficient and Lpa4-deficent mice display no obvious phenotypes [84,85], while cells from Lpa4-deficient mice display enhanced migration in response to LPA[85]. Mice deficient of both Lpa1 and Lpa2 present similar abnormities as knocking out Lpa1 alone with an increased incidence of frontal hematoma and lethality [78,84].

Effects of LPA on vascular smooth muscle cells

Phenotypic modulation of vascular SMCs occurs in response to vascular injury or consistent vascular pressure elevation [86,87]. Phenotypic modulation of SMCs involves their conversion from a normally quiescent, differentiated,

contractile state to a dedifferentiated state in which the cells proliferate, migrate and synthesize matrix proteins.

Isolated SMCs from human and rodent species can be stimulated to dedifferentiate, proliferate, and migrate by serum, and LPA has been proposed as one of the factors present in serum that may promote phenotypic modulation of vascular SMCs [88-90]. Indeed, isolated vascular SMCs respond to LPA by proliferating and migrating [91-93]. Although the specific LPA receptors and their signaling systems involved in SMC responses are not known, prominent pathways that are activated by LPA include Rho GTPases and extracellular-signal regulated kinase (ERK). LPA also regulates expression of early growth response-factor-1, a transcription factor, which stimulates expression of pro-inflammatory cytokines, adhesion molecules, growth factors, and coagulation factors [94]. LPA can promote tissue factor expression by SMCs [95], which may be a key component of the vascular wall involved in triggering thrombus formation [96]. Exogenous administration of LPA to animals elicits responses consistent with it serving as an endogenous mediator of vascular cell function. For example, intravenous injection of LPA elevates arterial blood pressure in rats [97] and local application causes cerebral vasoconstriction in pigs [98]. Moreover, local infusion of LPA in the rat common carotid artery induces vascular remodeling by stimulating neointimal

formation [99]. A similar response was observed in mice and was proposed to be mediated by PPAR γ [77].

The finding that LPA is capable of eliciting the development of intimal hyperplasia, which involves phenotypic modulation of SMCs, suggests that it may normally regulate SMCs, and our group have observed differences in the development of neointimal hyperplasia in mice lacking LPA1 receptor and in mice lacking both LPA1 and LPA2 in response to vascular injuries [100]. In the same study, we also established that neither LPA1 nor LPA2 was required for LPA to elicit a transient increase in blood pressure following intravenous administration of LPA to mice. Mice lacking both LPA1 and LPA2 responded similarly as wild-type (WT) mice in systemic blood pressure elevations in response to LPA infusion.

Effects of LPA on endothelial cells

LPA promotes endothelial cell migration through mechanisms that involve regulation of the actin cytoskeleton and the extracellular matrix [101,102]. LPA has been variably associated with increasing or decreasing endothelial barrier function but the inconsistencies between these sets of observations may arise from differences between the types of endothelial cells, the source of LPA, and the experimental approached used in these studies [103]. For example, several

investigators report that LPA stabilizes endothelial barrier function [104], decreases endothelial permeability [105], and increases endothelial resistance [106], whereas others have found that LPA promotes the loss of vascular integrity and decreases trans-endothelial resistance by preventing tight junction formation [107,108]. In lung injury models, vascular leak is mediated by the LPA1 receptor [109]. In cell culture systems, LPA triggers an inflammatory response in endothelial cells that includes up-regulation of expression of leukocyte chemoattractants [110] and adhesion receptors [111] in an LPA1 and LPA3- dependent manner [110 112]. These responses can regulate endothelial−leukocyte interactions by promoting monocyte binding to endothelial cells [111]. LPA also activates eNOS in endothelial cells [113] and may thereby regulate endothelial tone.

Effects of LPA in the lung

As discussed above, LPA has been shown to regulate contraction of other types of SMCs, such as aortic SMCs. In tracheal smooth muscle rings from both rabbits and cats, LPA alone does not cause contraction, but enhances the contractile response by methacholine [114]. This study was one of the first to suggest LPA's role in asthma, since asthmatic airways are hyperresponsive to contractile stimuli. The enhancement of contractility by LPA was not altered by removal of

epithelial cells, suggesting that LPA acts directly on SMCs, and the effect is independent of epithelial-derived mediators. The activation of Gi, Gq, and Rho were required for the effect [115,116]. LPA also strongly stimulate the proliferation of airway SMCs, and the mitogenic effect of LPA is completely blocked by pertussis toxin [117,118].

Airway epithelium is the first site of contact for inhaled particles and hence functions as a barrier to environmental stimuli. Recently He and colleagues reported LPA enhances the barrier integrity of pulmonary epithelial cells, and protects endotoxin-induced epithelial barrier disruption and lung injury. The effects of LPA are through PKCδ and PKCζ mediated E-cadherin accumulation at the cell-cell junctions. Their data suggest a protective role of LPA in airway inflammation and remodeling [119,120]. However, other studies showed pulmonary epithelial cells undergo rapid proliferation in response to LPA, which results in a transient decrease in inflammatory cytokines followed by an up-regulation of these cytokines that could lead to increased inflammation [121,122].

Pulmonary fibrosis begins as fibroblasts migrate into and fill up the airspace. The study by Tager and colleagues identified LPA as a key chemoattractant for lung fibroblasts after injury. LPA level increased in bronchoalveolar lavage fluid following bleomycin-induced lung injury in mice. Mice genetically deficient of

LPA1 were protected from fibrosis and mortality in this model. The absence of LPA1 led to reduced fibroblast recruitment and increased endothelial permeability, two responses that may be excessive in injuries that lead to fibrosis. In idiopathic pulmonary fibrosis patients, LPA levels in bronchoalveolar lavage fluid were also found to be increased. LPA1 antagonist markedly reduced responses of fibroblasts to the chemotactic activity of this fluid. Therefore LPA1 was identified as the receptor mediating LPA's chemoattractant effect in pulmonary fibrosis [109,123].

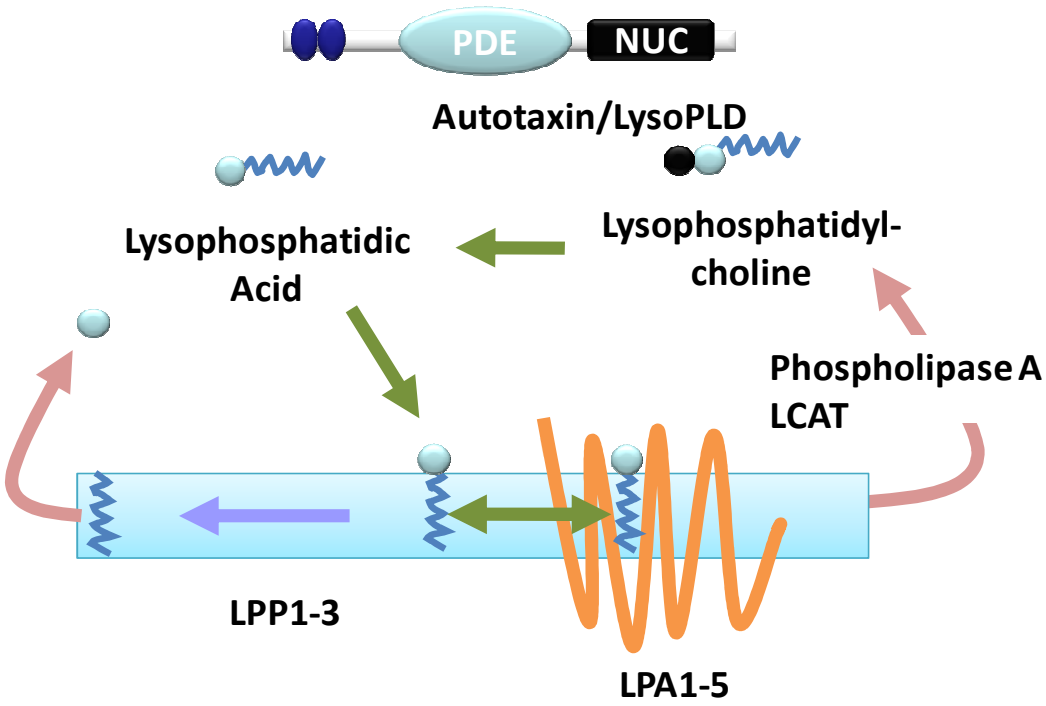

Figure 2.1. The production, degradation, and signaling of LPA.

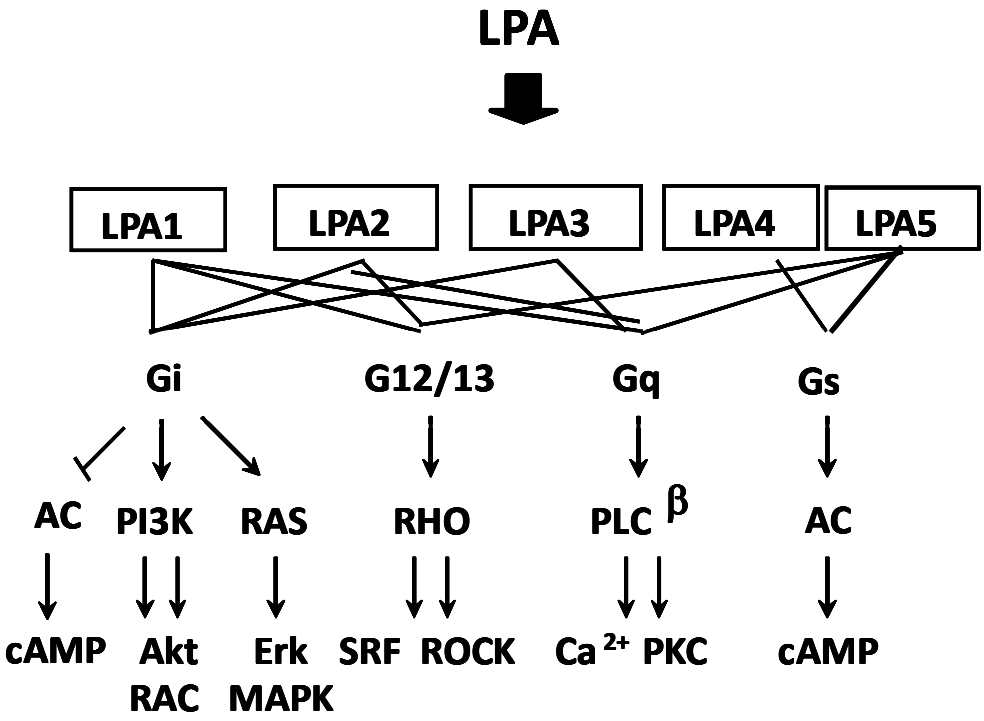

Figure 2.2. The signaling networks of LPA.

Chapter 3

Autotaxin/lysoPLD level regulates susceptibility to hypoxia-induced pulmonary hypertension in mice

Introduction

Arterial SMCs play an important role in vessel contraction and relaxation and, following systemic vascular injury, can undergo phenotypic modulation to a proliferative/synthetic state that likely contributes to the development of atherosclerosis and restenosis [100]. In the highly-compliant pulmonary circulation, which is characterized by high blood flow, low pressure, and low resistance, adaptations accommodate large changes in blood flow with little alteration of pressure. In particular, contraction of pulmonary vascular SMCs is tightly regulated by a balance between vasodilators and vasoconstrictors. When the balance fails, pulmonary arterial hypertension (PAH) ensues, with elevated pulmonary vascular resistance and sustained high pulmonary arterial pressure [22,27,29]. The main characteristics of PAH are vasoconstriction and vascular remodeling, including pulmonary vascular SMC proliferation and hypertrophy.

Additionally, endothelial dysfunction and in-situ thrombosis can occur [22,24,29]. Overtime, pressure overload of the right ventricle (RV) results in RV hypertrophy, dilatation, and dysfunction [22,124]. In fact, PAH is the leading cause of RV hypertrophy and failure [125]. Unfortunately, to date, very little is known about in initial establishment of PAH, making prevention and effective treatment challenging [28].

LPA is a bioactive lipid molecule present at physiologically relevant levels in plasma and serum [126]. The earliest evidence for biological activity of LPA came from studies demonstrating that it had pressor effects when administered to rats and guinea pigs[97] LPA had been proposed to contribute to phenotypic modulation of culture vascular SMCs and appears to modulate arterial remodeling responses in carotid arteries of rodents. LPA may also have important effects on endothelial cell function and endothelial barrier integrity [62,73,79].

The predominant route for LPA production in blood involves hydrolysis of LPC by the secreted plasma protein autotoxin/lysoPLD [64]. Autotaxin/lysoPLD is a member of the ectonucleotide pyrophosphatase/phosphodiesterase (ENPP) family and is designated ENPP2. The loss of autotaxin/lysoPLD in mice as a consequence of *Enpp2* gene deletion results in a much more striking phenotype than has been observed to date in any of the receptor knockout mice. Enpp2$^{-/-}$ mice

die embryonically and display vascular defects and vessel maturation failure [65,66]. Heterozygous *Enpp2* mice (Enpp2$^{+/-}$) exhibit no obvious developmental defect and have approximately half of normal circulating autotoxin/lysoPLD and LPA levels. Transgenic mice overexpressing human *Enpp2* have increased plasma autotoxin/lysoPLD activity and LPA levels [63]. These findings establish that autotoxin/lysoPLD plays an essential role in regulating circulating LPA levels in the blood and suggests that LPA may contribute to vascular development.

While substantial evidence suggests a role for LPA in regulating phenotypic modulation of cultured vascular SMCs and systemic arterial remodeling in rodent models, nothing is known about the effects of LPA on the pulmonary vasculature. In this chapter, we examined the role of LPA in regulation of the pulmonary vasculature using mice in which the autotaxin/LPA signaling axis is altered.

Chronic hypoxia is used extensively to induce experimental PAH in different animal species [36]. Mice exposed to sustained low oxygen environment first respond by vasoconstriction in the lung, and later develop pulmonary arterial remodeling and increased pulmonary resistance. SMC proliferation is one key characteristics of pulmonary vascular remodeling in response to sustained pressure elevation, and is usually assessed by increasing muscularized arterioles and thickening of the arteriolar wall. The sustained pressure elevation in the pulmonary vasculature in

turn elevates RV pressure and lowers the peak flow velocity across the pulmonary valve. The progression of pulmonary arterial hypertension in response to hypoxia is summarized in **Figure 3.1.** In this chapter, mice with decreased and elevated autotoxin/lysoPLD levels are subjected to hypoxia to induce experimental pulmonary hypertension. The development of PAH will be assessed by measuring RV systolic pressure, peak flow velocity across the pulmonary valve, and muscularization percentage of pulmonary arterioles.

Materials and Methods

Mice

All procedures conformed to the recommendations of *Guide for the Care and Use of Laboratory Animals* (Department of Health, Education, and Welfare publication number NIH 78-23, 1996) and were approved by the Institutional Animal Care and Use Committee. Generation and characterization of Enpp2$^{+/-}$ and Enpp2-Tg were as previously described [66] [63]. The Enpp2$^{+/-}$ and Enpp2-Tg are back-crossed to FVB background. Mice were housed in cages with HEPA filtered air in rooms on 12-hour light cycles and fed Purina 5058 rodent chow ad libitum.

Hypoxia model

Mice were exposed to oxygen-poor air (hypoxia) at normal atmospheric pressure by

placement of their cages in a commercially available chamber (A-chamber, BioSpherix). The mice resided in the chamber for 24 hrs per day for 3 weeks to induce pulmonary hypertension and vascular remodeling, and were removed from the chamber only for cage, food, and water changes. The hypoxic environment within the chamber was achieved by inflow of compressed nitrogen gas. The oxygen concentration (FIO_2 = 0.10) was controlled by a commercially available oxygen controller (Proox model 110, BioSpherix). Prior and after 3 weeks of hypoxia treatment, echocardiography was performed to evaluate the cardiac function. RV pressures measurements were performed in both normoxic and hypoxic groups. Mice were then euthanized, and organs were collected for histological, biochemical, and gene expression analysis.

Echocardiography

Transthoracic echocardiography was performed using a 30 MHz probe and the Vevo 770 Ultrasonograph (VisualSonics). Mice were lightly anesthetized with 0.8 % isoflurane, maintaining heart rate at 400–500 beats/min. The hair was removed from the chest using a chemical hair remover (Nair®). The heart rate and body temperature were maintained and recorded. Two-dimensional parasternal long- and short-axis views were obtained. M-mode tracings were recorded and used to determine LV end-diastolic diameter (LVEDD) and LV end-systolic diameter

(LVESD). LV fractional shortening (FS) was calculated using the formula %FS = (LVEDD - LVESD) / (LVEDD). For determining the flow across the pulmonary valve, high short-axis view was obtained at the level of the right ventricular outflow tract and in which the pulmonary valve can be easily seen. The Doppler mode cursor was positioned at the end of the pulmonary valve to record the peak velocity across the pulmonary valve.

RV pressure measurement

Under anesthesia (inhaled isoflurane 1 – 3%), the mouse was fixed in a supine position with tape on a mouse pad that has imbedded EKG electrodes and surface mounted semi-conductor temperature sensor that distributes heat through surface mounted resistors. Rectal temperature was monitored. Under direct visualization of the trachea, an endotracheal tube was inserted and connected to a Harvard rodent volume-cycled ventilator (Model 645, Harvard Apparatus) via the Y-shaped connector. Ventilation was performed with a tidal volume of 200 μL and a respiratory rate of 150/min. Oxygen was provided to the inflow of the ventilator. The chest cavity was opened by an incision of the left fourth intercostal space. An 1 French catheter (Millar Instruments) was quickly inserted into the RV and pressure traces was obtained by Chart 5 Pro (AD Instruments). The animal was euthanized while still under anesthesia, and organs were obtained for histology and RT-PCR

analysis.

Real-time PCR

Total RNA was extracted from tissues and primary cultured cells using Trizol (Invitrogen) following manufacturer's instructions. cDNA was prepared with Multiscribe reverse-trasncriptase enzyme as per manufacturer's directions (High-Capacity cDNA Archive Kit; Applied Biosystems). mRNA expression was measured by real-time quantitative PCR using TaqMan® gene expression assays (Applied Biosystems) in an ABI Prism® 7500 Fast Real-Time PCR System. Threshold cycles (C_T) were determined by an in-program algorithm assigning a fluorescence baseline based on readings prior to exponential amplification. Fold change in expression was calculated using the $2^{-\delta\delta CT}$ method. 18s ribosomal RNA was used as an endogenous control.

Histology

Mice were weighed, and hearts, lungs, livers, and kidneys were dissected, rinsed in PBS, and weighed. Hearts were cut in a cross section at the widest point. The top half of the heart was fixed with 4% paraformaldehyde and embedded in paraffin. 5 μm sections of hearts and lungs were prepared with microtome. The sections were stained with hematoxylin and eosin (H&E) for examination of gross appearance, whereas Masson's Trichrome, periodic acid-Schiff (PAS), counterstained with

hematoxylin (PAS-H), and van Gieson elastin staining was employed to facilitate quantification of fibrosis, cardiomyocyte size, and elastin content respectively. The muscularization percentage of small arterioles was quantified with lung sections immunostained with the biotinylated anti- α-smooth muscle actin antibody (Sigma). The dilution fold of the antibody was 1 to 100 in PBS. Small arterioles with diameters ranging in 15-100 μm were scored. Arterioles with no positive α-smooth muscle actin staining were characterized as non-muscularized, wrapped with 0-75% positive staining as partially-muscularized, and >75% positive staining as fully-muscularized vessels. 50 arterioles in each section were counted.

Statistics

All results were expressed as mean ± SD. In vitro studies were repeated a minimum of 3 times, and results were analyzed by Student *t* test or ANOVA. Statistical significance within strains was determined using ANOVA with multiple pair-wise comparisons. Statistical analysis was performed using Sigma-STAT software version 3.5 (Systat Software Inc). A probability value of less than 0.05 was considered significant.

Results

Reduction in autotaxin/lysoPLD promotes hypoxia-induced pulmonary

remodeling in mice

LPA has been proposed to play a role in phenotypic modulation of cultured vascular SMCs and may regulate systemic arterial remodeling in experimental models. However, nothing is known about the effects of LPA on the pulmonary vasculature. To explore the role of LPA in the pulmonary vasculature, mice with reduced and elevated levels of the autotoxin/lysoPLD, the major LPA producing enzyme, were exposed to oxygen-poor air (hypoxia) for 3 weeks. In response to hypoxia, pulmonary vasoconstriction occurs and is followed by remodeling of the pulmonary vasculature. In wild-type (WT) mice, hypoxia results in an increase in pulmonary arterial pressure, which can be monitored by measuring right ventricular systolic pressure (RVSP) by insertion of a pressure catheter directly into the right ventricle. Following hypoxia exposure (FiO_2=0.1), an increase of RVSP occurs in WT mice (30.3 ± 2.3 mmHg; n =6) compared to RVSP in age-matched normoxic littermates (25.7 ± 2.1 mmHg; n =6) **(Figure 3.2)**.

To determine if LPA contributes to pulmonary remodeling, we subjected mice with varying levels of LPA to hypoxia. Inherited deficiency of autotaxin/lysoPLD ($Enpp2^{-/-}$) in mice results in embryonic lethality by E10.5 due to vascular defects [65,66], heterozygous $Enpp2^{+/-}$ mice have reduce LPA levels, but are viable with no obvious vascular developmental abnormalities. Likewise, $Enpp2^{+/-}$

mice display similar RVSP (23.8 ±1.8 mmHg; n =5) under normoxic conditions as their WT littermates. Following a 3-week exposure to hypoxia, Enpp2$^{+/-}$ mice developed higher RVSP (36.2 ± 5.2 mmHg; n=7) then did their WT littermates (30.3 ± 2.3 mmHg; n =6) **(Figure 3.2)**. Although the difference of RVSP values was not statistically significant between hypoxic Enpp2$^{+/-}$ mice and WT littermates, we noticed that the difference of RVSP was significant between normoxic and hypoxic Enpp2$^{+/-}$ mice, while it was not statistically significant between normoxic and hypoxic WT groups. Therefore Enpp2$^{+/-}$ mice seemed to show greater reaction to hypoxia-induced RVSP elevation.

The peak flow velocity across the pulmonary valve was measured by echocardiography as an indication of RV stroke volume before (baseline) and after 3 weeks of treatments (normoxia or hypoxia). Peak flow velocity across the pulmonary valve decreased by 8.0 ± 5.7% ($P<0.05$) following hypoxia in WT mice **(Table 3.1)**. The decline in peak flow velocity was approximately twice as great (16.2 ± 8.4%; $P<0.05$) in Enpp2$^{+/-}$ littermates after exposure to hypoxia **(Table 3.1)**. Taken together, the greater increase in RVSP and decline in peak flow velocity across the pulmonary valve suggest Enpp2$^{+/-}$ mice are more sensitive to hypoxia-induced pulmonary vasoconstriction and hypertension. We also calculated the pulmonary velocity acceleration time from the echocardiography. However,

although used to monitor PAH in human, we could not see a significant difference between normoxic and hypoxic conditions. Therefore, the peak flow velocity between the pulmonary valves seems to be a more sensitive method to evaluate PAH in our case. The LV fractional shortening percentage was also obtained by echocardiography to verify whether the overall cardiac function was affected by hypoxia treatment. No significant change was found between baseline and post-treatments (data not shown).

To confirm that the changes in RVSP and peak flow velocity reflect differences in pulmonary vascular remodeling, muscularization of small pulmonary arterioles in response to hypoxia was examined. Lung sections stained with α-smooth muscle actin, a marker for SMCs, were scored for non-, partially, and fully- muscularized small pulmonary arterioles. The pulmonary histology of $Enpp2^{+/-}$ mice was not notably different from WT controls at baseline. In particular, WT and $Enpp2^{+/-}$ littermates maintained in normal conditions did not differ in the percentage of non- or fully muscularized arterioles. Following a 3-week exposure to hypoxia, an increase in the percentage of fully muscularized small arterioles occurred in WT mice, confirming the pulmonary vascular remodeling in our hypoxia model. Relative to the WT controls, lungs from $Enpp2^{+/-}$ mice exposed to hypoxia had a higher percentage of fully-muscularized and a lower percentage of

non-muscularized distal small arterioles then did WT controls **(Figure 3.3)**. The differences in pulmonary arteriolar muscularization percentage were statistically significant between hypoxic Enpp2$^{+/-}$ and WT controls (82% muscularized arterioles in Enpp2$^{+/-}$ mice versus 68.5% in WT mice; $P<0.05$). By all parameters, Enpp2$^{+/-}$ mice seemed to have exaggerated pulmonary vascular responses to hypoxia that was consistent with an augmentation in hypoxia-induced pulmonary hypertension.

The expression level of Enpp2 in the lung among different groups was examined by quantitative RT-PCR. As expected based on our previous findings of lower autotoxin/lysoPLD protein level in the lungs of Enpp2$^{+/-}$ mice [63], Enpp2 mRNA expression in lungs of Enpp2$^{+/-}$ mice was 20% of that in lungs from WT littermates. No significant change in gene expression of Enpp2 occurred after hypoxia in either Enpp2$^{+/-}$ mice and WT littermates **(Figure 3.4)**. The expression level of LPA receptors in the lung was also measured. The lack of significant increase of Lpa1-5 in Enpp2$^{+/-}$ mice to WT littermates in both normoxic and hypoxic conditions suggests no compensatory up-regulation of LPA receptors in response to decreased Enpp2 level in the lung. On the contrary, levels of Lpa1-5 were slightly but consistently lower in Enpp2$^{+/-}$ mice to WT in normoxic condition. Following exposure to hypoxia, while no obvious change in the expression patterns

of Lpa1-3 was seen, pulmonary Lpa4 and Lpa5 gene expression were consistently reduced in mice of both strains when compared to the normoxic groups, with Lpa4 levels declining by 20 - 50% and Lpa5 levels by 30 - 40%. No obvious compensatory changes in other LPA receptors were observed with hypoxia exposure **(Figure 3.5)**.

Hypoxia-induced pulmonary remodeling in mice with increased autotaxin/lysoPLD and LPA levels

Transgenic overexpression of Enpp2 in mice (Enpp2-Tg) increases plasma lysoPLD activity and LPA levels [63]. To determine if increases in circulating LPA levels might protect from hypoxia-induced pulmonary hypertension, Enpp2-Tg and age-matched WT control mice were subjected to 3 weeks of hypoxia. At baseline, Enpp2-Tg mice display normal RVSP (25.1 ± 6.9 mmHg; n =8) . RVSP increase following hypoxia in Enpp2-Tg was not significantly lower from WT control mice (33.8 ± 5.7 mmHg; n =9 for Enpp2-Tg versus 37.0 ± 5.1 mmHg; n =8 for WT) **(Figure. 3.6)**. Although there was no significant difference in RVSP, Enpp2-Tg mice did display less decline in peak flow velocity across the pulmonary valve. Peak flow velocity across the pulmonary valve decreased by 15.6 ± 8.7% following hypoxia in WT mice. The decline in peak flow velocity was less (4.4 ± 6.8%; not

statistically significant) in Enpp2-Tg mice after exposure to hypoxia **(Table 3.2)**. Together, our data suggest Enpp2-Tg mice may be protected from hypoxia-induced pulmonary hypertension, but the protective effect is rather moderate when comparing to the hypersensitivity of $Enpp2^{+/-}$ mice.

Muscularization of small pulmonary arterioles in response to hypoxia was again used as an indicator for pulmonary vascular remodeling. The percentage of distal arteriolar muscularization was very similar in WT and Enpp2-Tg mice post hypoxia (86.5% muscularized arterioles in Enpp2-Tg mice versus 83% in WT mice; not statistically significant) **(Figure 3.7)**. However, interestingly, the percentage of muscularized arterioles was statistically higher in Enpp2-Tg mice to age-matched WT controls in normoxic condition (74.5% muscularized arterioles in Enpp2-Tg mice versus 42% in WT mice; $P<0.05$). Hence, the increase in arteriolar muscularization was very limited in Enpp2-Tg mice exposed to hypoxia. Enpp2-Tg mice seemed to be more resistant to hypoxia-induced pulmonary arteriolar remodeling. Taken together, Enpp2-Tg mice may display a moderate protective effect toward hypoxia-induced pulmonary hypertension.

Expression of the human Enpp2 transgene is driven by the α1-anti-trypsin inhibitor promoter, which may result in expression in the lung. Therefore, primers specifically recognizing human Enpp2 mRNA were used to determine the

expression level of the transgene. As expected, no human Enpp2 mRNA was detected in lung of WT mice. The exposure of Enpp2-Tg mice to hypoxia is associated with an approximately 50% reduction in human Enpp2 mRNA levels **(Figure 3.8A)**, which may account for the lack of a significant phenotype in the transgenic mice with hypoxia. There was no significant change of endogenous mouse Enpp2 mRNA level between WT and Enpp2-Tg in both normoxic and hypoxic conditions **(Figure 3.8B)**. However, like human Enpp2 transgene, the expression of endogenous Enpp2 also decreased by 30% ~ 50% with hypoxia.

mRNA levels of LPA receptors in the lung were measured to see whether their expression was affected by increased autotoxin/lysoPLD and LPA levels or hypoxia. Expression levels of Lpa1, 2, 4, and 5 were the same in Enpp2-Tg and age-matched WT mice, while Lpa3 was consistently lower in Enpp2-Tg mice. This indicates expression of Lpa3 may be down-regulated by excess LPA in the circulation. Following hypoxia, Lpa4 and Lpa5 declined in both WT and Enpp2-Tg mice while levels of other receptors remained relatively the same. Overall, no significant difference in receptor expression levels was found to suggest a role of specific receptors in hypoxia-induced pulmonary hypertension **(Figure 3.9)**.

Since Enpp2$^{+/-}$ and Enpp2-Tg mice react differently to hypoxia-induced pulmonary hypertension, we also tested whether these mice spontaneously develop

pulmonary hypertension at different ages. As shown earlier, RVSP of young adult (2-3 months old) Enpp2$^{+/-}$ and Enpp2-Tg mice does not differ from their age-matched WT controls **(Figure 3.2 and 3.6).** In aged group (6 months and older), Enpp2$^{+/-}$ and Enpp2-Tg mice also displayed RVSP values in the normal range, and did not differ from their age-matched WT controls (data not shown). Therefore, we concluded Enpp2$^{+/-}$ and Enpp2-Tg mice did not spontaneously develop pulmonary hypertension without hypoxia stimulation.

Discussion

In this chapter, we aimed to determine the regulatory effect of LPA in the pulmonary vasculature. Hypoxia was used as a challenge to pulmonary vasculature, and the reactivity of mice with genetically altered expression of autotoxin/lysoPLD and LPA levels to hypoxia was examined.

Mice were exposed to half of the normal oxygen concentration at normal atmospheric pressure for 3 weeks to induce pulmonary hypertension. The oxygen concentration and duration of our hypoxic condition was based on previous studies [36]. The success of hypoxia-induced pulmonary hypertension was determined by increase in RVSP, decrease in peak flow velocity across the pulmonary valve, and increase of muscularized pulmonary arterioles in hypoxic WT animals, comparing

to littermates raised in room air (normoxia).

Genetic manipulation that reduces the expression of autotoxin/lysoPLD and decreases circulating LPA levels in mice, promotes the development of pulmonary hypertension with hypoxia. Thus, LPA may play a protective role by preventing hypoxia-induced pulmonary vasoconstriction. In contrast, mice overexpressing human autotaxin/lysoPLD may be mildly protected from hypoxia-induced changes, as suggested by preservation of peak flow velocity across the pulmonary valve. The moderate phenotype of the Enpp2-Tg mice may be limited by down-regulation of transgene expression that occurs during hypoxia and would be expected to reduce LPA levels. Moreover, autotoxin/lysoPLD and LPA at physiologically normal levels may be sufficient for the protective effect, and further increases may provide no additional benefit. The fact that Enpp2-Tg mice show less reduction in peak flow velocity across the pulmonary valve, but no significant difference in RVSP to age-matched WT controls after hypoxia also suggests that the reduction in pulmonary flow is a more sensitive parameter that is subjected to change earlier in the progression of pulmonary hypertension.

The percentages of muscularized arterioles in hypoxic condition were similar in Enpp2-Tg and control mice. However, interestingly, Enpp2-Tg mice showed a much higher percentage of muscularized vessels at baseline (normoxia) to

age-matched WT mice. We could not explain the possible mechanism behind it, and no abnormality in the overall pulmonary histology of Enpp2-Tg mice was found (data not shown). Nevertheless, the higher percentage of muscularized arterioles at baseline made the increase in muscularization after hypoxia very limited, if any, in Enpp2-Tg mice. In the sense, Enpp2-Tg mice seem to be more resistant to pulmonary vascular remodeling with hypoxia exposure.

Enpp2$^{+/-}$ mice are bred by crossing Enpp2$^{+/-}$ and WT littermates, and therefore the control group is their WT littermates. The Enpp2-Tg colony is bred from the original Enpp2-Tg line, and their control group is age-matched WT mice from the same background. Enpp2$^{+/-}$ and Enpp2-Tg mice are both in the FVB background. Interestingly, the two WT groups show certain differences at baseline as well as responses to hypoxia. The RVSP values at normoxia were similar (25.7 $\pm$ 2.1 mmHg of WT for Enpp2$^{+/-}$ and 24.9 $\pm$ 3.0 mmHg of WT for Enpp2-Tg). However, the WT for Enpp2-Tg had a higher RVSP value after hypoxia (37.0 $\pm$ 5.1 mmHg versus 30.2 $\pm$ 2.3 mmHg of WT for Enpp2$^{+/-}$). WT for Enpp2-Tg also showed ~2 fold more reduction in peak flow velocity across the pulmonary valve after hypoxia (-15.6 $\pm$ 8.7 % versus -8.0 $\pm$ 5.7 % of WT for Enpp2$^{+/-}$). As to pulmonary vascular remodeling, the muscularization percentages of 2 WT groups were similar at baseline. However, in the hypoxic group, the percentage of

non-muscularized arterioles was 32% in WT for Enpp2$^{+/-}$ and only 17% in WT for Enpp2-Tg. Overall, by all parameter looked, the WT for Enpp2-Tg showed exacerbated response toward hypoxia. The differential responses can be attributed to strain variations. Although both Enpp2$^{+/-}$ and Enpp2-Tg mice are on the FVB background, the Enpp2-Tg are the on the FVB/NJ background, and the Enpp2$^{+/-}$ mice are the European FVB sub-strain, which was transferred from the US to Amsterdam in 1978. The two sub-strains are kept separately for decades, and therefore there may be genetic drifts between the FVB/NJ mice and the FVB line used in Europe that could account for the differential responses. In addition, the WT littermates for Enpp2$^{+/-}$ mice are congenic which were back-crossed at least 10 times to FVB background, while the WT used for Enpp2-Tg are isogenic FVB mice. The SV-129 genes left in the congenic mice may account for the differential responses. Nevertheless, the baseline values of RVSP and peak flow velocity across the pulmonary valve were similar between Enpp2$^{+/-}$, Enpp2-Tg and their respective WT controls.

In this chapter, we demonstrate a novel role for LPA in the regulation of pulmonary vasculature. By studying mouse models with elevated and reduced LPA levels, our data suggest that circulating LPA levels are necessary for the maintenance of normal pulmonary vascular tone. The next question is how LPA

signaling regulates the pulmonary vasculature and which receptor(s) mediate the effect. The expression levels of Lpa 1-5 in the lung are measured. The expression of Lpa4 and 5 were down-regulated with hypoxia in all strains (Enpp2$^{+/-}$, Enpp2-Tg and their respective WT controls). No obvious compensatory expression in any specific genotypes upon treatment was found. Therefore, the specific receptor(s) mediating the protective effect of LPA to pulmonary hypertension remains to be determined.

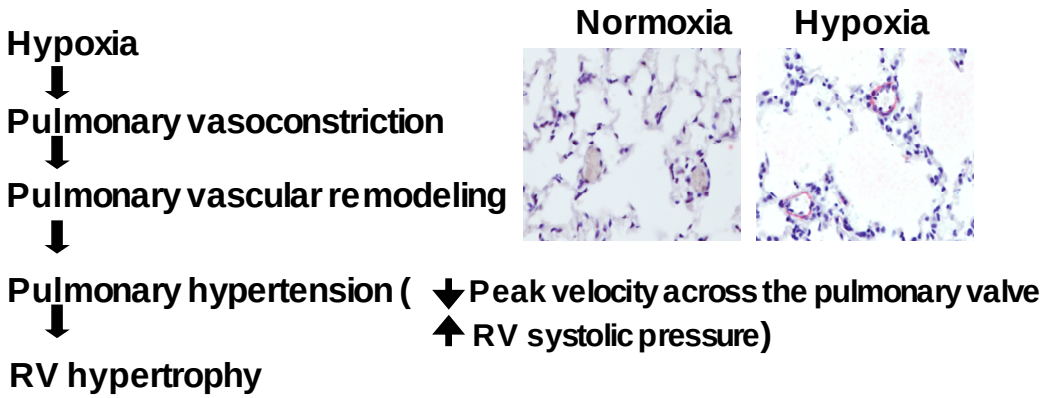

Figure 3.1. Progression of hypoxia-induced pulmonary hypertension .
Lungs sections from normoxic and hypoxic mice were stained with α-smooth muscle actin (red) to show increased muscularization and wall thickness of pulmonary arterioles as signs of pulmonary remodeling in the hypoxic group.

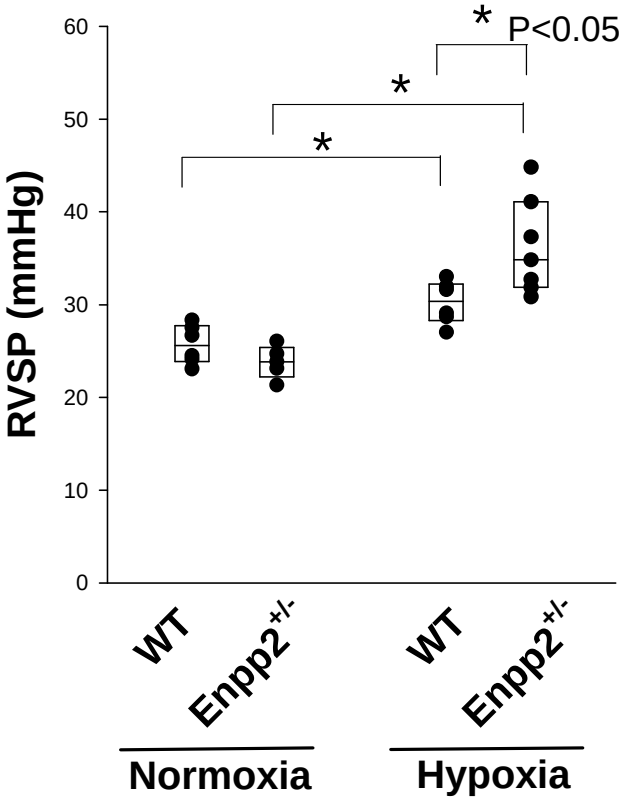

Figure 3.2. The response of mice with reduced ATX levels ($Enpp2^{+/-}$) to hypoxia.

Right ventricular systolic pressure (RVSP) of WT (n=6) and $Enpp2^{+/-}$ (n=5) mice in normoxia, and WT (n=6) and $Enpp2^{+/-}$ (n=7) mice 3 weeks with hypoxia. Individual values (dots) and medium with 25 and 75 confidence intervals (box plots) are presented. Data were analyzed by 2-way ANOVA. *P<0.05.

Genotype	Condition	N	Before	After
WT	**Normoxia**	4	878.79 ± 44.38	993.05 ± 69.58
WT	**Hypoxia**	6	898.85 ± 76.3	824.52 ± 55.3
Enpp2$^{+/-}$	**Normoxia**	5	927.71 ± 65.61	922.96 ± 41.22
Enpp2$^{+/-}$	**Hypoxia**	7	960.68 ± 92.91	802.29 ± 94.79

Results are presented as mean ± SD in mm/sec.

Table 3.1. Peak flow velocity across the pulmonary valve before and after 3 weeks of exposure to normoxia or hypoxia.

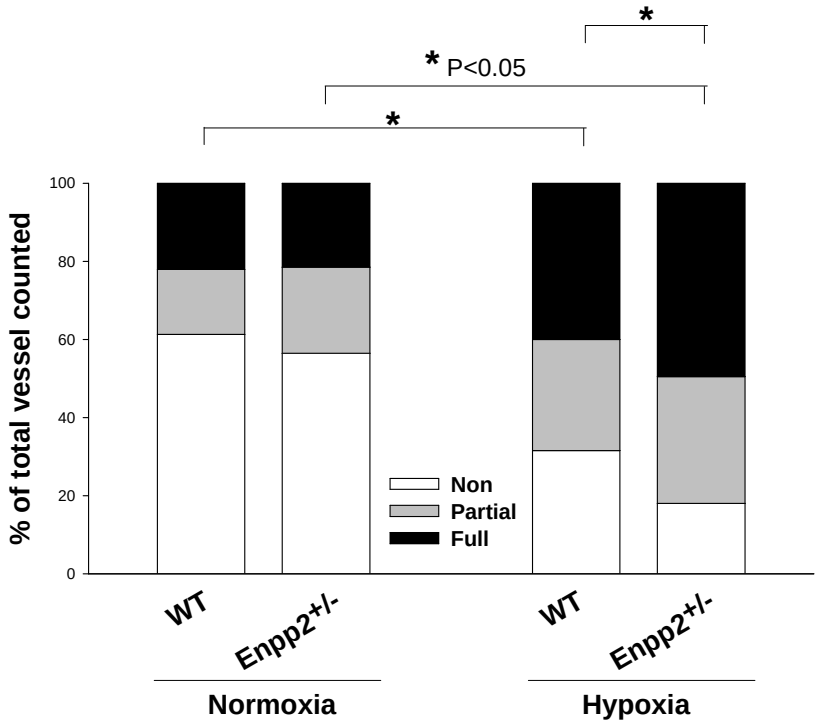

Figure 3.3. Percentages of muscularization of distal pulmonary arterioles in normoxic or hypoxic WT and Enpp2$^{+/-}$ mice.

Lung sections were immunostained with α-smooth muscle actin and scored as described in Materials and Methods. non= non muscularized vessels, partial= partially muscularized vessels, and full= fully muscularized vessels. Data are presented as averages of 4 mice/group and analyzed by 2-way ANOVA. *P<0.05.

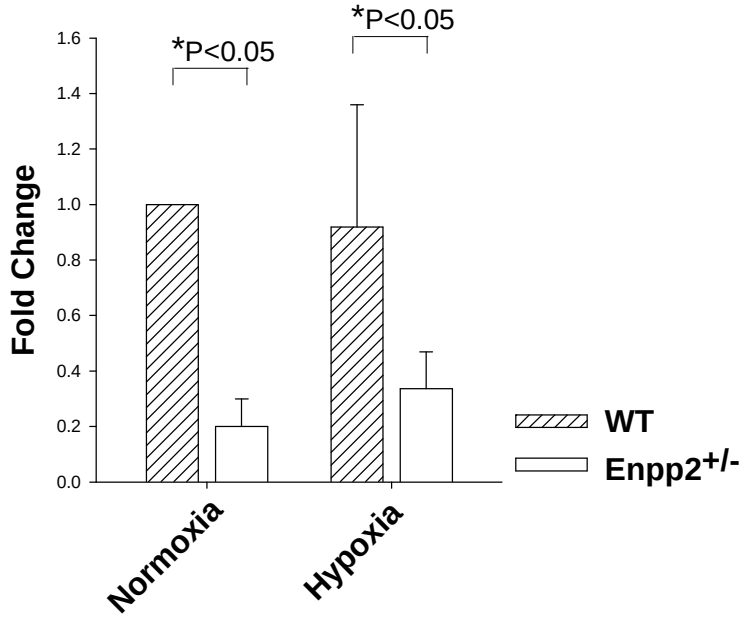

Figure 3.4. ATX expression level in lung of mice with lowered ATX levels (Enpp2$^{+/-}$) with hypoxia.

Quantitative RT-PCR analysis of autotaxin/lysoPLD (ATX) expression level in lung of littermates of WT (slashed bars) and Enpp2$^{+/-}$ (open bars) mice in normoxic and hypoxic conditions. All Results were graphed from four experiments and presented as mean ± S.D. The expression level from WT mice in normoxic condition is set as 1. *P<0.05 .

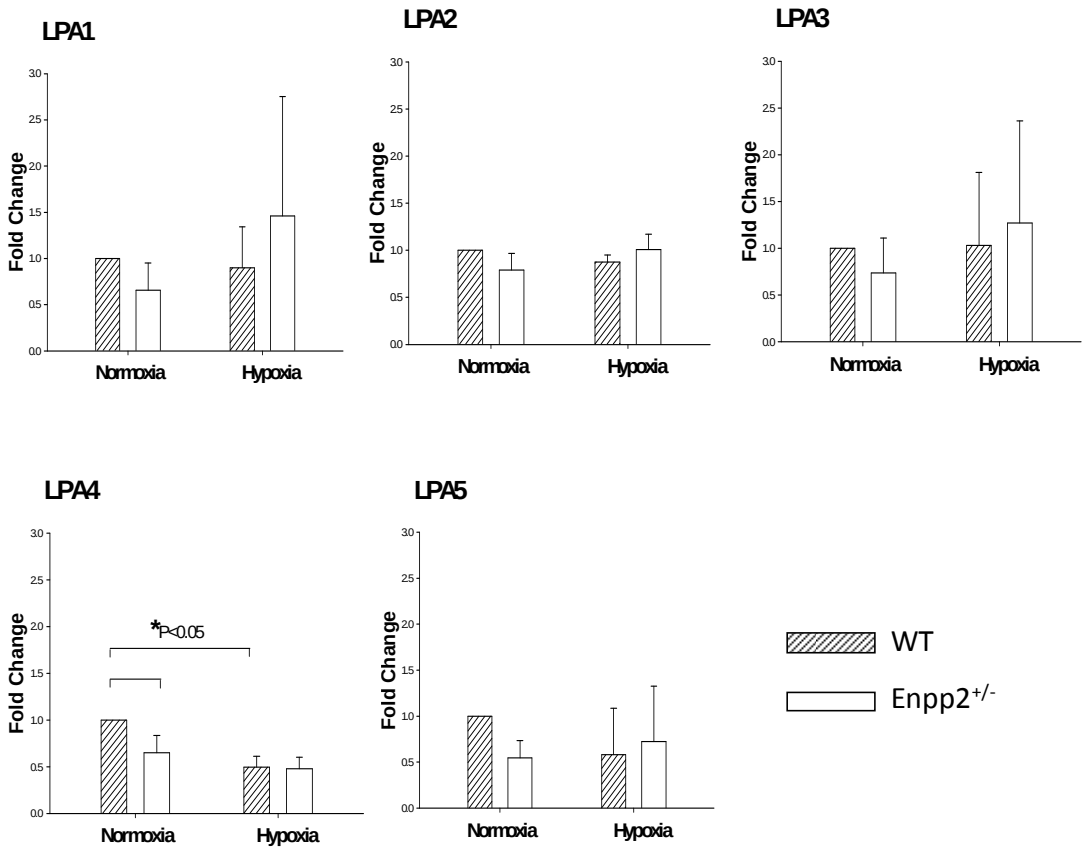

Figure 3.5. Expression level of LPA receptors in the lung of Enpp2$^{+/-}$ mice.

Quantitative RT-PCR analysis of LPA1-5 expression level in lung of littermates of WT (slashed bars) and Enpp2$^{+/-}$ (open bars) mice in normoxic and hypoxic conditions. All results were graphed from four experiments and presented as mean ± S.D. The expression level of WT mice in normoxic condition is set as 1. *P<0.05 .

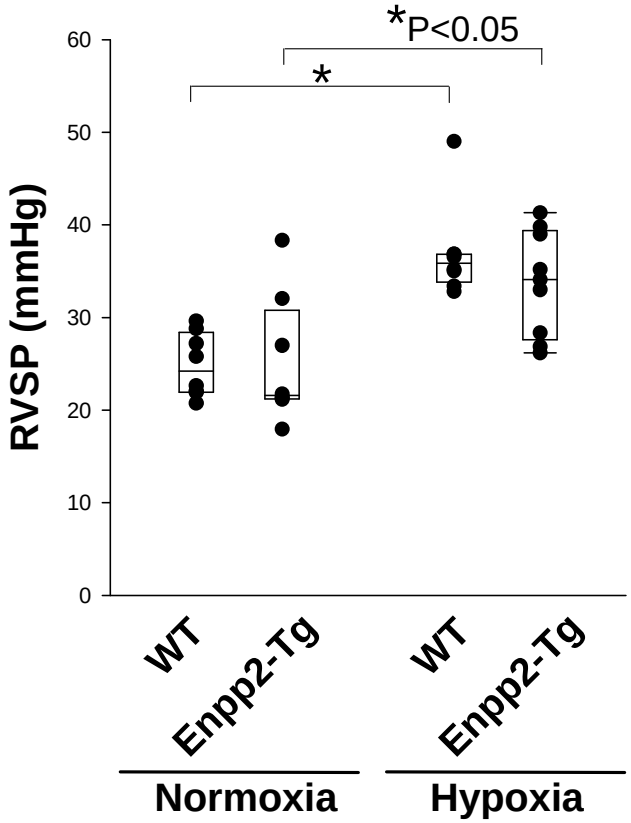

Figure 3.6. The response of mice with elevated ATX levels (Enpp2-Tg) to hypoxia.

Right ventricular systolic pressure (RVSP) of WT (n=8) and Enpp2-Tg (n=8) mice in normoxia, and of WT (n=8) and Enpp2-Tg (n=9) mice 3 weeks with hypoxia. N=8 for both WT and Enpp2-Tg mice in normoxia. N=8for WT and 9 for Enpp2-Tg mice in hypoxia. Individual values (dots) and medium with 25 and 75 confidence intervals (box plots) are presented. Data were analyzed by 2-way ANOVA. *P<0.05.

Genotype	Condition	N	Before	After
WT	**Normoxia**	5	1004.28 ± 43.89	946.70 ± 60.08
WT	**Hypoxia**	5	963.81 ± 64.84	808.30 ± 38.42
Enpp2-Tg	**Normoxia**	5	1040.56 ± 41.54	1026.97 ± 51.09
Enpp2-Tg	**Hypoxia**	5	1018.06 ± 111.29	967.09 ± 57.34

Results are presented as mean ± SD in mm/sec.

Table 3.2. Peak flow velocity across the pulmonary valve of mice before and after 3 weeks of exposure to normoxia and hypoxia.

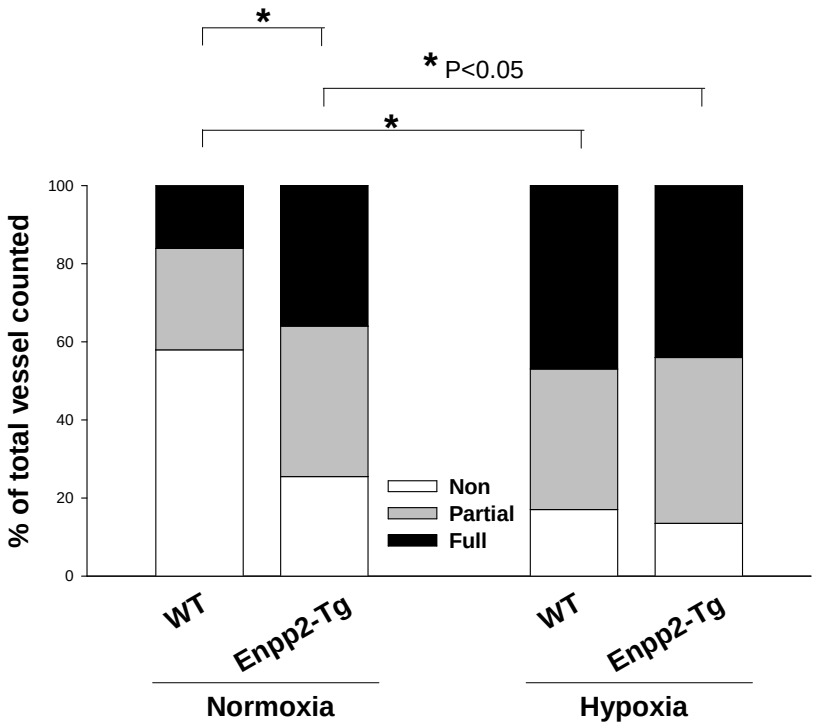

Figure 3.7. Muscularization of distal pulmonary arterioles in normoxic or hypoxic WT and Enpp2-Tg mice.

Lung sections were immunostained with α-smooth muscle actin and scored as described in Materials and Methods. Data are presented as averages of 4 mice/group and analyzed by 2-way ANOVA. *P<0.05.

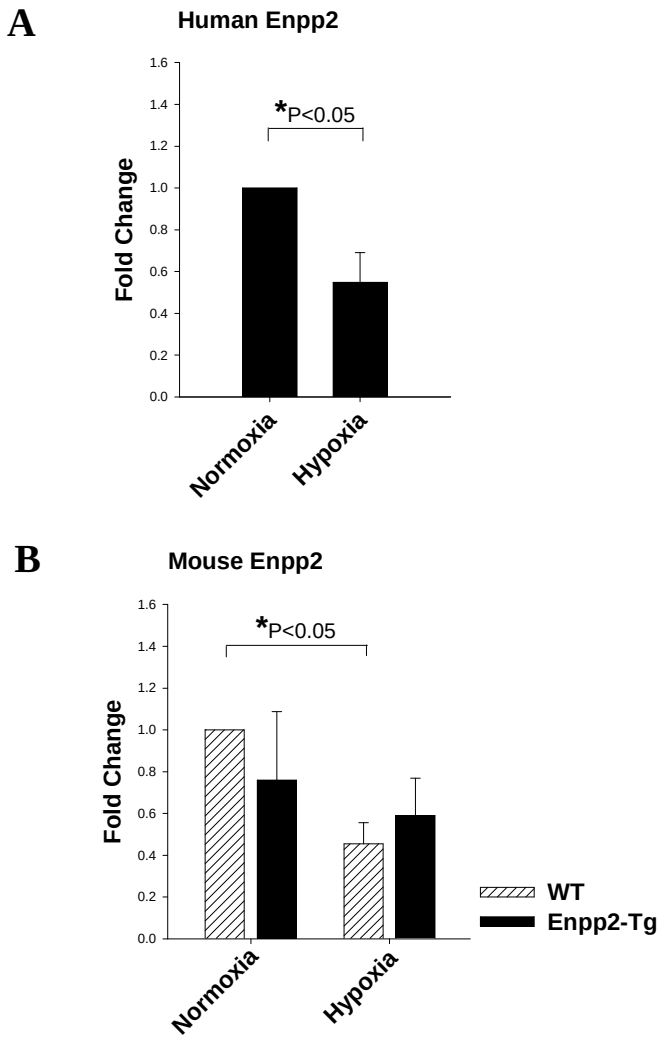

Figure 3.8. ATX expression level in lung of mice with elevated ATX levels (ATX-Tg) with hypoxia exposure.

A. Quantitative RT-PCR analysis of human ATX transgene expression level in lung of ATX-Tg (closed bars) mice in normoxic and hypoxic conditions.

B. Quantitative RT-PCR analysis of endogenous mouse ATX expression level in lung of age-matched WT (slashed bars) and Enpp2-Tg (closed bars) mice in normoxic and hypoxic conditions.

All Results were graphed from four experiments and presented as mean ± S.D. The expression level from WT mice in normoxic condition is set as 1.

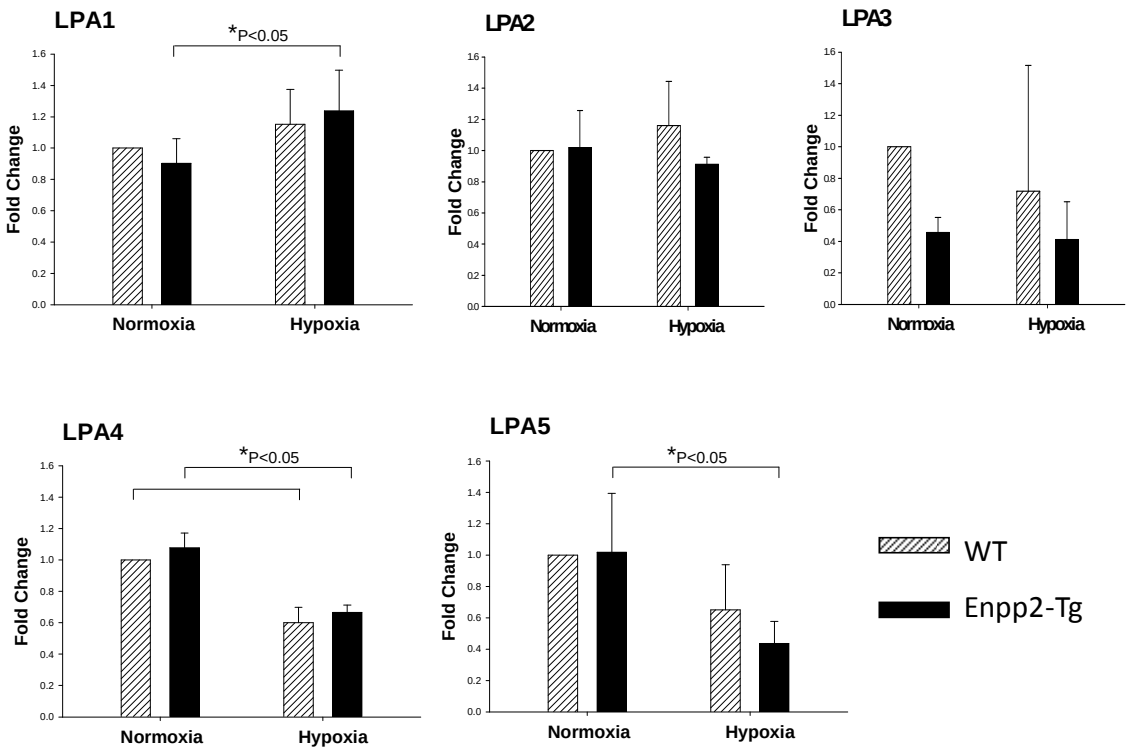

Figure 3.9. Expression levels of LPA receptors in lung of Enpp2-Tg mice.

Quantitative RT-PCR analysis of LPA1-5 expression level in lung of littermates of WT (slashed bars) and Enpp2-Tg (closed bars) mice in normoxic and hypoxic conditions. All results were graphed from four experiments and presented as mean ± S.D. The expression level of WT mice in normoxic condition is set as 1. *P<0.05.

Chapter 4

LPA receptors 1 and 2 in pulmonary vascular regulation

Introduction

A family of G protein-coupled receptors (GPCRs) is at least partially responsible for the cellular responses of LPA. At present, there are five bona fide LPA receptors, LPA1-5 [62,73], with evidence for at least three more (LPA 6 – 8)[74,75]. LPA receptors 1 – 5 are expressed ubiquitously in most mammalian tissues. *In vitro* studies in cell lines reveal that LPA receptors share certain function redundancy as well as specificity [62,79,80]. Until recently, understanding the physiologic role of these receptors has been hampered by lack of subtype specific, selective receptor agonists and antagonists. However, genetic deletion of LPA receptors has provided valuable information on their pathophysiological roles [127]. For example, deficiency of Lpa1 in mice generates craniofacial abnormalities, reduced size, a small incidence of perinatal frontal hematoma, and 50% neonatal lethality [81], whereas deletion of Lpa3 results in implantation defects[82,83]. Lpa2-deficient and Lpa4-deficent mice display no obvious phenotypes [84,85], although cells from

Lpa4-deficient mice display enhanced migration in response to LPA[85]. Mice deficient of both Lpa1 and Lpa2 present similar abnormities as knocking out Lpa1 alone except an increased incidence of frontal hematoma [84].

LPA is an effective modulator in the cardiovascular system. Its production is facilitated by activated platelets, and it has multiple effects on vascular SMCs and endothelial cells. For example, LPA is well-known for its phenotypic modulating effect on cultured vascular SMCs by promoting their de-differentiation, proliferation, and migration [88-90]. LPA promotes endothelial cell migration that involves organization of the actin cytoskeleton and the extracellular matrix [101,102]. LPA has been variably reported to increase or decrease endothelial barrier function [103]. By using quantitative RT-PCR analysis, others and our lab had established that LPA1 and LPA2 expressed relatively high levels in vascular SMCs and endothelial cells [128,129]. Given that LPA is poised to be a mediator of vascular disease, we are interested in characterizing the vascular phenotype of mice lacking LPA receptors 1 and 2 ($LPA1^{-/-}2^{-/-}$ mice) [84].

To date, not much has been reported regarding the cardiovascular and pulmonary-related phenotypes of $LPA1^{-/-}2^{-/-}$ mice. Our group recently reported the roles of LPA1 and LPA2 in regulation of phenotypic modulation of vascular SMCs after injury [100]. $LPA1^{-/-}2^{-/-}$ mice were partially protected from developing carotid

ligation and femoral artery denudation-induced neointimal hyperplasia, whereas LPA1$^{-/-}$ mice developed larger neointimal lesions after injury. The injury-induced response of LPA2$^{-/-}$ mice was similar to that of WT mice. Growth in serum, LPA-induced extracellular signal-regulated ERK activation, and migration to LPA and serum were all attenuated in SMCs isolated from LPA1$^{-/-}$2$^{-/-}$ mice. In contrast, LPA1$^{-/-}$ SMCs exhibited enhanced migration resulting from an up-regulation of LPA3. However, despite their involvement in intimal hyperplasia, neither LPA1 nor LPA2 was required for dedifferentiation of SMCs following vascular injury or dedifferentiation of isolated SMCs in response to LPA or serum in vitro. Similarly, neither LPA1 nor LPA2 was required for the transient increase in systemic blood pressure following intravenous administration of LPA to mice. These results identify a role for LPA1 and LPA2 in regulating SMC migratory responses in the context of vascular injury.

In bleomycin-induced lung injury models, endothelial permeability is mediated by the LPA1 receptor [109]. Pulmonary fibrosis was markedly inhibited in LPA1$^{-/-}$ mice, and these mice were protected from mortality after bleomycin treatment. The lack of LPA1 led to reduced fibroblast recruitment. LPA levels in bronchoalveolar lavage fluid were increased, and inhibition of LPA1 significantly reduced fibroblast responses to the chemotactic activity in idiopathic pulmonary

fibrosis patients.

Given our preliminary data of the protective effect of LPA on hypoxia-induced pulmonary hypertension, and the high expression levels of LPA1 and LPA2 in endothelial and SMCs, we sought to determine whether LPA1 and LPA2 participate in the regulatory effect of LPA in the pulmonary vasculature.

Materials and Methods

Mice

All procedures conformed to the recommendations of *Guide for the Care and Use of Laboratory Animals* (Department of Health, Education, and Welfare publication number NIH 78-23, 1996) and were approved by the Institutional Animal Care and Use Committee. Generation and characterization of $LPA1^{-/-}2^{-/-}$ mice were as previously described [81,84]. The $LPA1^{-/-}2^{-/-}$ mice were backcrossed for >10 generations to the Balb/c background. Mice were housed in cages with HEPA filtered air in rooms on 12-hour light cycles and fed Purina 5058 rodent chow ad libitum.

Hypoxia model

This method was stated in chapter 3.

Echocardiography

This method was stated in chapter 3.

RV pressure measurement

This method was stated in chapter 3.

Real-time PCR

This method was stated in chapter 3.

Histology

Mice were weighed, and hearts, lungs, livers, and kidneys were dissected, rinsed in PBS, and weighed. Hearts were cut in a cross section at the widest point. The top half of the heart was fixed with 4% paraformaldehyde and embedded in paraffin. 5 μm sections of hearts and lungs were prepared with microtome. The sections were stained with hematoxylin and eosin (H&E) for examination of gross appearance, whereas Masson's Trichrome, periodic acid-Schiff, counterstained with hematoxylin (PAS-H), and van Gieson elastin staining was employed to facilitate quantification of fibrosis, cardiomyocyte size, and elastin content respectively. Thickness of LV and RV free walls and total cross-section diameter of the heart was measured at the level of LV papillary muscles in H&E stained sections. Measurements were made at 3 individual sites and averaged [130,131]. Cardiomyocyte hypertrophy was assessed by measuring cross-sectional area of 50 cardiomyocytes with nearly circular capillary profiles and centered nuclei in randomly selected

fields in the LV or RV free walls per PAS-H-stained section.[132] To perverse the pulmonary architecture, lungs were tracheal perfused with 4% paraformaldehyde at 25cm pressure for 10 minutes in some cases. [133] The morphology, muscularization percentage of small arterioles, and arteriolar wall thickness were quantified with lung sections immunostained with the biotinylated anti- α-smooth muscle actin antibody (Sigma). The dilution of the antibody was 1 to 100 in PBS. Small arterioles with diameters ranging in 15-100 μm were scored. Arterioles with no positive α-smooth muscle actin staining were characterized as non-muscularized, wrapped with 0-75% positive staining as partially-muscularized, and >75% positive staining as fully-muscularized vessels. 50 arterioles in each section were counted for muscularization percentage. For quantification of pulmonary vascular wall thickness, pictures of small arterioles with diameters ranging in 15-100 μm are taken and analyze with Metamorph image software. The outer and inner diameter of each arterioles are measured, and the arteriolar wall thickness was calculated by the formula: wall thickness was calculated as (outer vessel circumference/2π) – (circumference of lumen/2π) [134]. 25 arterioles in each section were quantified for pulmonary vascular wall thickness. Van Gieson elastin staining was used to stain elastin and collagen in the lung sections. Perivascular elastin deposition was quantified by the density of positive elastin staining on the vascular wall and

normalized by vascular diameters using Metamorph image software.

Oxygen saturation

Mice were lightly anesthetized with isoflurane. The real-time oxygen saturation of arterial hemoglobin, heart rate, pulse distension, breath distension, and respiratory rate were obtained and analyzed with mouseOx (Starr) by placing a sensor on the right thigh of the mouse.

Hematological analysis

Retro-orbital bleeding was performed with mice anesthetized with isoflurane. Whole blood was collected into EDTA-coated tubes. Hemoglobin concentration and hematocrit were analyzed with ABC vet hematology analyzer (ABX) set to measure mouse blood cell parameters.

Pulmonary vascular permeability

Mice were kept anesthetized with pentobarbital. The neck skin was cut open, and 1% Evans blue in PBS was injected into the right jugular vein (100μl / mice). 15 minutes later, heparin with PBS was perfused from RV to LV at a constant rate of 111.8 ml/hr (25 mmHg pressure). The perfused lung was dissected, weighed and immersed in 1ml formamide to extract Evans blue. The extraction was performed in a shaking water bath at 56° C for 24 hours. The extracted Evans blue was quantified by reading absorbance at 600 nm and normalized to lung weight.

Statistics

This method was stated in chapter 3.

Results

LPA1$^{-/-}$2$^{-/-}$ mice develop pulmonary hypertension with age

In chapter 3, we found that mice with reduced circulating autotoxin/lysoPLD and LPA levels (Enpp2$^{+/-}$ mice) are prone to develop pulmonary hypertension with hypoxia exposure. LPA receptors 1 and 2 were reported to be abundantly expressed in cultured endothelial and vascular SMCs, and we observed relatively high expression levels in murine blood vessels. We therefore were interested in understanding whether these 2 receptors are involved in regulating the pulmonary vasculature.

Young LPA1$^{-/-}$2$^{-/-}$ mice (8 – 14 weeks old) did not display a significant increase in RVSP when comparing to age-matched WT controls (37.9 ± 8.8 mmHg in LPA1$^{-/-}$2$^{-/-}$ mice versus 28.6 ± 8.0 mmHg in WT mice; not statistically significant) **(Figure 4.1A)**. When measuring RVSP in aged mice (over 45 weeks old), we observed a significant increase in pressures of LPA1$^{-/-}$2$^{-/-}$ mice when comparing to WT mice (58.5 ± 4.5 in LPA1$^{-/-}$2$^{-/-}$ mice versus 28.6 ± 8.0 mmHg in WT mice; $P<0.05$) that did not occur in mice singly deficient of LPA1 (LPA1$^{-/-}$) or LPA2

(LPA2$^{-/-}$) **(Figure 4.1B)**.

In agreement with the age-dependent elevation in RVSP observed in LPA1$^{-/-}$2$^{-/-}$ mice, peak flow velocity across the pulmonary valve was 11% lower in LPA1$^{-/-}$2$^{-/-}$ (613 ± 125 mm/sec; n = 18) than in WT (690 ± 94 mm/sec; n= 22; not statistically significant) mice at 2 – 3 months of age. The decline became more evident with age, as the peak flow velocity was 18% lower in the LPA1$^{-/-}$2$^{-/-}$ mice (573 ± 70 mm/sec; n = 14) than WT controls (698 ± 92 mm/sec; n=11; $P<0.05$) by 6 – 9 months of age, **(Table 4.1)**. In comparison to the decline in peak flow velocity in LPA1$^{-/-}$2$^{-/-}$ mice over time, the WT mice in two age groups displayed almost the same values. Taken together, our findings indicate LPA1$^{-/-}$2$^{-/-}$ mice develop spontaneous pulmonary hypertension with age.

To determine whether the elevation of RVSP was reflected in histology, we examined the heart cross-sections of aged WT and LPA1$^{-/-}$2$^{-/-}$ mice for RV hypertrophy. The RV free wall was notably thicker, and RV chamber was dilated in the representative pictures of LPA1$^{-/-}$2$^{-/-}$ heart to age-matched WT controls **(Figure 4.2A)**. Quantification showed significantly higher RV free wall thickness to cross-section diameter ratio of aged LPA1$^{-/-}$2$^{-/-}$ mice (0.17 ± 0.05) comparing to age-matched WT mice (0.10 ± 0.02; $P<0.05$). There was no difference among WT and single knockout mice (LPA1$^{-/-}$ and LPA2$^{-/-}$mice) **(Figure 4.2B)**.

To confirm the thickening of RV free wall was due to RV hypertrophy, we measured the cross-section area of individual cardiomyocytes and numbers of nuclei per microscopic field in RV and LV of aged WT and $LPA1^{-/-}2^{-/-}$ heart sections. Average cardiomyocyte size was significantly greater in RV of $LPA1^{-/-}2^{-/-}$ mice comparing to WT controls (179 ± 57% in $LPA1^{-/-}2^{-/-}$ RV versus 100 ± 5% in WT RV; $P<0.05$), while the nuclei numbers per field stayed the same. Cardiomyocyte size and nuclei numbers were very similar in LV of both genotypes, indicating the size increase of cardiomyocyte happened specifically in RV **(Figure 4.3)**. Hence, we confirmed that in agreement with the increase in RVSP, the $LPA1^{-/-}2^{-/-}$ mice developed RV hypertrophy with age. No histological evidence of cardiac fibrosis or inflammation was found in the $LPA1^{-/-}2^{-/-}$ heart sections. Taken together, these physiological and histological changes further confirmed the development of pulmonary hypertension in $LPA1^{-/-}2^{-/-}$ mice with age.

To look for the possible mechanism of the spontaneous development of pulmonary hypertension, we examined parameters that cause secondary pulmonary hypertension. We excluded hypoxia as a cause for pulmonary hypertension in the $LPA1^{-/-}2^{-/-}$ mice. Arterial oxygen saturation in WT mice were 96 ± 1% and 97 ± 1% at 1 - 2 months and 6 months of age, respectively. Corresponding values in the $LPA1^{-/-}2^{-/-}$ mice were 95 ± 2%, 97 ± 0.3% and 96 ± 2% at 1 - 2 months, 3 –

4 months and >6 months of age, respectively **(Figure 4.4A)**. Additionally, hemoglobin (17.6 ± 1.3 g/dl) and hematocrit values (53.3 ± 4.4 %) in $LPA1^{-/-}2^{-/-}$ mice did not differ from age-matched WT (17.4 ±1.6 g/dl and 55.3 ± 7.9 %), indicating that the $LPA1^{-/-}2^{-/-}$ mice did not develop secondary polycythemia, which would be expected to occur in the setting of prolonged hypoxia **(Figure 4.4B and C)**. We also examined whether pulmonary vascular permeability was changed in $LPA1^{-/-}2^{-/-}$ mice. Evans Blue dye was injected into the jugular vein of WT and $LPA1^{-/-}2^{-/-}$ mice. After perfusion the pulmonary circulation at physiological relevant pressure, Evans blue leaked into the lung tissue was extracted and quantified. The average amount of extracted Evans Blue was the same in WT and $LPA1^{-/-}2^{-/-}$ mice, suggesting normal permeability of the pulmonary vasculature in $LPA1^{-/-}2^{-/-}$ mice (0.9 ± 0.3 in $LPA1^{-/-}2^{-/-}$ mice versus 1.0 ± 0.4 in WT mice) **(Figure 4.5A)**. In accordance to normal pulmonary permeability, no evidence of edema was seen in the lung tissue of $LPA1^{-/-}2^{-/-}$ mice. Examination of pulmonary valves did not reveal any notable abnormalities of $LPA1^{-/-}2^{-/-}$ mice, excluding pulmonary stenosis as a cause for the elevated RVSP **(Figure 4.5B)**. Plastic casting and microCT analysis of the pulmonary vasculature also did not reveal obvious obstruction in the main pulmonary vasculature (data not shown).

Abnormal pulmonary development in LPA1$^{-/-}$2$^{-/-}$ mice

Normal pulmonary vascular formation is critical for lung alveolarization, which requires coordinated growth and differentiation of pneumocytes, endothelial cells and vascular SMCs. In mice, the final stage of lung development occurs postnatally, when primary air saccules divide into smaller air spaces through the process of secondary septation [1,2]. When we analyzed lung sections for the pulmonary vascular remodeling, we noted enlarged alveoli in the lung section of LPA1$^{-/-}$2$^{-/-}$ mice, and sought to characterize their pulmonary development more carefully. Histological examination of the lung sections from 12-week old LPA1$^{-/-}$2$^{-/-}$ mice revealed an increase in the size of alveolar space. The process of alveolar septation in mice is largely complete by 3 weeks of age, at which time alveolar enlargement was already present in LPA1$^{-/-}$2$^{-/-}$ mice **(Figure 4.6)**. At 3 weeks of age, there was an increase in the muscularization of pulmonary arterioles in LPA1$^{-/-}$2$^{-/-}$ mice comparing to age-matched WT controls (preliminary data; n=2), and the increased muscularization became more evident at 12 weeks (63% muscularized arterioles in LPA1$^{-/-}$2$^{-/-}$ mice versus 18% in WT mice; $P<0.05$) **(Figure 4.8A)**. Histological examination of lung sections at postnatal day 3 (P3) and 7 (P7) did not reveal any obvious changes in the lung architecture in LPA1$^{-/-}$2$^{-/-}$ mice, and therefore the impairment of lung development was likely to

occur between P7 and P21. **(Figure 4.6)**.

Because the level of elastin, one of the major ECM components in the lung, may affect normal lung development as well as vascular pressure, we measured elastin gene expression (*Eln*) in lungs of LPA1$^{-/-}$2$^{-/-}$ mice, and found that *Eln* expression was 1.9 ±0.37 fold in LPA1$^{-/-}$2$^{-/-}$ than in WT controls. At 3 weeks of age, LPA1$^{-/-}$2$^{-/-}$ mice had a similar 2-fold elevation of *Eln* as compared to WT controls **(Figure 4.7A)**. To determine whether the up-regulation of *Eln* is reflected in elastin deposition, elastin staining of lung sections was performed. Representative pictures show increased black elastin staining surrounding vessels of various sizes in the lungs of LPA1$^{-/-}$2$^{-/-}$ mice **(Figure 4.7C)**. Quantification of elastin content around the vessels confirmed greater perivascular elastin deposition in LPA1$^{-/-}$2$^{-/-}$ mice at both 3 and 12 weeks of age (1.7 ± 0.2 fold increase for 3 weeks old and 2.5 ± 0.6 fold increase for 12 weeks old LPA1$^{-/-}$2$^{-/-}$ mice) **(Figure 4.7B)**.

Enhanced hypoxia-induced pulmonary remodeling in mice with deficiency of LPA1 and LPA2 receptors

Having acknowledged that aged LPA1$^{-/-}$2$^{-/-}$ mice had increased RVSP, we hypothesized that LPA1$^{-/-}$2$^{-/-}$ mice may be susceptible to hypoxia-induced

pulmonary hypertension and remodeling as were mice with reduced LPA level (Enpp2$^{+/-}$). Young LPA1$^{-/-}$2$^{-/-}$ mice (8 – 14 weeks old) did not display a significant increase in RVSP when comparing to age-matched WT controls **(Figure 4.1A)** and were subjected to hypoxia for 3 weeks. Similar to Enpp2$^{+/-}$ mice, an approximately 2-fold reduction in peak flow velocity across the pulmonary valve occurred in LPA1$^{-/-}$2$^{-/-}$ mice after hypoxia (25.3 ± 16.9% of LPA1$^{-/-}$2$^{-/-}$ mice versus 13.8 ± 16.3% of WT mice; not statistically significant) **(Table 4.2)**.

Muscularization of small pulmonary arterioles was used to confirm that the changes in peak flow velocity reflected in pulmonary vascular remodeling in response to hypoxia. In agreement with the finding that LPA1$^{-/-}$2$^{-/-}$ mice develop greater decline in peak flow velocity across the pulmonary valve, analysis of the lungs revealed more muscularized and less non-muscularized pulmonary arterioles in LPA1$^{-/-}$ 2$^{-/-}$ mice as compared to age-matched WT controls in response to 3-week exposure to hypoxia (86.5% muscularized arterioles in LPA1$^{-/-}$2$^{-/-}$ mice versus 53% in WT mice; $P<0.05$) **(Figure 4.8A)**. Proliferation of vascular SMCs not only increases the percentage of muscularized small arterioles, but also increases the thickness of vascular wall. Consistent with the increase in the number of muscularized arterioles, the average thickness of pulmonary arteriolar wall was significantly higher in LPA1$^{-/-}$2$^{-/-}$ mice than WT controls with hypoxia treatment

(Figure 4.8B). Interestingly, the fact that LPA1$^{-/-}$2$^{-/-}$ mice had less non-muscularized and more muscularized vessels, as well as thicker pulmonary arteriolar wall to WT controls in normoxia revealed more pulmonary vascular remodeling of LPA1$^{-/-}$2$^{-/-}$ mice at baseline **(Figure 4.8)**. This implies that there may be certain degree of defect in the pulmonary vasculature of LPA1$^{-/-}$2$^{-/-}$ mice prior to any stimulation. Similar to elevated RVSP with age, the absence of LPA1 and LPA2 may be associated with spontaneous pulmonary arterial remodeling.

Sustained elevation in RVSP stimulates RV hypertrophy with increases in cardiomyocyte mass and RV free wall thickness. **Figure 4.9A** shows representative pictures of heart cross-sections of WT and LPA1$^{-/-}$2$^{-/-}$ mice in normoxic and hypoxic conditions. A thicker RV free wall was observed in the hypoxic LPA1$^{-/-}$2$^{-/-}$ heart. Quantification of heart cross-sections revealed increase in the RV free wall thickness to total cross-section diameter in both WT and LPA1$^{-/-}$2$^{-/-}$ mice after hypoxia, indicating our model of hypoxia-induced pulmonary hypertension was sufficient to trigger RV hypertrophy **(Figure 4.9B)**. Higher RV free wall thickness to cross-section diameter ratio of LPA1$^{-/-}$2$^{-/-}$ mice to WT controls in normoxia indicate the spontaneous development of RV hypertrophy of LPA1$^{-/-}$2$^{-/-}$ mice. Together, LPA1$^{-/-}$2$^{-/-}$ mice showed greater decline in peak flow velocity, more muscularization and increased pulmonary arteriolar wall thickness,

and RV hypertrophy with hypoxia treatment. These findings suggest that mice with impaired LPA signaling with lack of LPA1 and 2 are hyper-responsive to hypoxia-induced pulmonary hypertension.

We measured gene expression levels of LPA receptors 1 - 5 in lungs of mice to determine if their expression was altered in the absence of LPA1 and LPA2. As expected, no Lpa1 or Lpa2 gene expression in lungs from $LPA1^{-/-}2^{-/-}$ mice could be detected. The expression levels of Lpa4 and Lpa5 were higher in $LPA1^{-/-}2^{-/-}$ to WT lung at baseline, but not as obvious with hypoxia exposure. Interestingly, the up-regulation of Lpa3 mRNA level that was observed in WT controls following exposure to hypoxia did not occur in the lungs of $LPA1^{-/-}2^{-/-}$ mice **(Figure 4.10)**.

Discussion

In this chapter, we found $LPA1^{-/-}2^{-/-}$ mice developed spontaneous pulmonary hypertension with age. While the RVSP of young adult $LPA1^{-/-}2^{-/-}$ and WT mice showed no obvious difference, the RVSP of aged $LPA1^{-/-}2^{-/-}$ mice was significantly elevated than age-matched WT controls mice (58.5 ± 4.5 in $LPA1^{-/-}2^{-/-}$ mice versus 28.6 ± 8.0 mmHg in WT mice, $p<0.05$). $LPA1^{-/-}$ mice may also display a slightly higher RVSP than WT controls, but the difference was not significant. Lacking LPA1 may have partial effect on the age-dependent

development of pulmonary hypertension. Nevertheless, neither LPA1$^{-/-}$ and LPA2$^{-/-}$ mice display the significant elevation of RVSP observed in the LPA1$^{-/-}$2$^{-/-}$ mice, suggesting redundant signaling pathways between these two receptors. The spontaneous development of pulmonary hypertension in aged LPA1$^{-/-}$2$^{-/-}$ mice was further confirmed by decline in peak flow velocity across the pulmonary valve as well as RV hypertrophy.

No obvious compensatory up-regulation of other LPA receptors was found in the lungs of LPA1$^{-/-}$2$^{-/-}$ mice. The higher expression levels of Lpa4 and 5 in normoxic LPA1$^{-/-}$2$^{-/-}$ mice were not seen in the hypoxic group. Interestingly, the up-regulation of Lpa3 in hypoxic WT mice was not seen in hypoxic LPA1$^{-/-}$2$^{-/-}$ mice, indicating LPA3 might also participate in the responses to hypoxia, and lacking certain LPA receptors, such as LPA1 and LPA2 in this case, may affect the signaling of other receptors.

After establishing that LPA1$^{-/-}$2$^{-/-}$ mice were susceptible to hypoxia-induced pulmonary remodeling and develop spontaneous pulmonary hypertension with age, we sought to determine the possible cause(s). As discussed earlier, chronic hypoxia contribute to pulmonary hypertension, and therefore we first checked the arterial oxygen saturation percentage at various ages. The oxygen saturation of LPA1$^{-/-}$2$^{-/-}$ mice was within the normal range from 6 to 36 weeks old. In addition,

markers for prolonged hypoxia, such as increase in hemoglobin and hematocrit values were not seen in LPA1$^{-/-}$2$^{-/-}$ mice. We therefore excluded hypoxia as the cause.

Valvular diseases and obstruction in the pulmonary vasculature could also lead to pulmonary hypertension. By examining tissue sections, we did not find signs for pulmonary valve stenosis or other histological evidence to suggest valvular disease as a likely cause for pulmonary hypertension. The lack of pulmonary valve stenosis was further supported by the fact that LPA1$^{-/-}$2$^{-/-}$ mice showed decreased peak flow velocity across the pulmonary valve rather than increase, which would be expected in the case of pulmonary valve stenosis. No architectural defect in the main pulmonary vasculature was noted by plastic casting and microCT analysis (data not shown). Examination of the lung tissue sections also failed to find evidences for thromboembolism or cor pulmonale.

Endothelial cell plays a key role in the regulation of pulmonary vascular tone by balancing the vasoconstrictive and vasodilatory factors, and therefore endothelial dysfunction could contribute to pulmonary hypertension. To determine the integrity of the endothelial layer, we checked the pulmonary endothelial permeability by measuring the leakage of Evans blue dye into the lung tissue. No significant increase in pulmonary endothelial permeability was found in LPA1$^{-/-}$2$^{-/-}$

mice. We also challenged age-matched WT and LPA1$^{-/-}$2$^{-/-}$ mice with hypoxia and performed the permeability assay. No difference was found in hypoxia-challenged mice either (data not shown). However, interestingly, we did not see an increase in pulmonary permeability with hypoxia exposure as other groups reported. This could be attributed to different hypoxia conditions, such as the hypobaric hypoxia model used by other groups [135,136]. Another explanation is that we could not perform the pulmonary permeability assay in the hypoxic environment. Therefore, the endothelial layer could revert to normal shortly after the mice were taken out from the hypoxic chamber, so that we were not able to detect the change in time. Transmission electron microscopy was performed for a detailed look of the pulmonary endothelial cells, and the lining of endothelium appeared to be intact in the lung of LPA1$^{-/-}$2$^{-/-}$ mice (data not shown).

Overall, no striking histological changes, such as fibrosis, inflammation, and edema, were found in the lung and heart of LPA1$^{-/-}$2$^{-/-}$ mice. Therefore the cause for the pulmonary hypertension may be more subtle and molecular-based effect rather than architectural changes of the pulmonary vasculature.

While looking for histological evidences, we noticed enlarged alveoli in the lung of LPA1$^{-/-}$2$^{-/-}$ mice. We therefore fixed the alveolar structure by paraformaldehyde perfusion through trachea and confirmed the enlargement of

alveoli in LPA1$^{-/-}$2$^{-/-}$ mice at both 3 and 12 weeks of age. Since murine pulmonary development is not complete until 3 weeks after birth, the lack of LPA1 and 2 may likely result in impaired alveolarization, rather than disruption of the existing alveoli such as that occurs with emphysema. No evident difference at postnatal day 3 and 7 were seen in the lung architecture of LPA1$^{-/-}$2$^{-/-}$ mice, suggesting the impairment of pulmonary development likely occurred between postnatal day 7 and 21, the time of alveolar septation in mice.

The disrupted pulmonary development in LPA1$^{-/-}$2$^{-/-}$ mice may be associated with the development of pulmonary hypertension. The percentages of muscularized arterioles were higher in both 3 and 12 weeks old LPA1$^{-/-}$2$^{-/-}$ mice, comparing to age-matched WT controls, suggesting the vascular remodeling was evident as early as 3 weeks of age (50% of muscularized vessels in LPA1$^{-/-}$2$^{-/-}$ mice versus 30% in WT mice). The difference in 12 weeks old mice was even greater (63% in LPA1$^{-/-}$2$^{-/-}$ mice versus 18% in WT mice), indicating the progression of vascular remodeling with age. The pulmonary histology of LPA1$^{-/-}$ and LPA2$^{-/-}$ mice appears to be normal without alveolar enlargement. This again suggested the redundancy of these receptors in the regulation of pulmonary vasculature (data not shown). To determine whether lacking LPA 1 and 2 in mice affects other vascular beds, we performed fundoscopy test to examine the retinal

microvasculature of LPA1$^{-/-}$2$^{-/-}$ and WT mice. No notable difference was found in the retinal microvasculature, suggesting the changes in the pulmonary vasculature were unique (data not shown).

Adequate composition and cross-linking of extracellular matrix (ECM) are keys to the development as well as maintenance of the vascular tone in the pulmonary vasculature [137]. Since elastin is the major ECM component of mammalian lung [138], we sought to determine whether the elastin deposition was affected in LPA1$^{-/-}$2$^{-/-}$ mice. LPA1$^{-/-}$2$^{-/-}$ mice expressed higher level of *eln* at both 3 and 12 weeks of age. In accordance to gene expression, the perivascular elastin content was also higher in these mice. Perivascular elastin deposition is tightly associated with hypertension. Increased elastin deposition was reported to occur in the arterial wall together with or very shortly after blood pressure elevation, and the deposition was proportional to pressure elevation [139]. On the other hand, studies have shown that increased elastin deposition could be the cause rather than the consequence for hypertension. Baccarini-Contri and colleagues found that augmented elastin deposition occurred in young spontaneously hypertensive rats (SHR) before full establishment of hypertension, and even in fetal and neonatal rats [140]. Briones and colleagues further incubated isolated SHR arteries with elastase to degrade elastin, and found the elastase incubation reversed the

structural and mechanical alterations of the arteries that were remodeled due to hypertension [141]. We did not know whether the increase of elastin was the cause of pulmonary hypertension, or simply a reflection of the high arterial pressure in LPA1$^{-/-}$2$^{-/-}$ mice. If impaired LPA signaling results in increased elastin expression, which leads to pulmonary hypertension, we would expect to see down-regulation of *eln* expression by activation of LPA signaling. However, our preliminary cell culture data suggest that LPA stimulates *eln* expression in primary cultured pulmonary arterial SMCs. Therefore the up-regulation of *eln* in LPA1$^{-/-}$2$^{-/-}$ mice may reflect the increase in pulmonary arterial and/or abnormal vascular development in the LPA1$^{-/-}$2$^{-/-}$ mice.

As in chapter 3, we also used hypoxia as a model to test the pulmonary vascular reactivity. We found signaling through LPA1 and LPA2 may mediate the effect of LPA in the regulation of pulmonary vasculature, as mice lacking both receptors were more susceptible to hypoxia-induced pulmonary remodeling and the development of pulmonary arterial hypertension, characterized by declined peak flow velocity across the pulmonary valve, increased pulmonary arteriolar muscularization and wall thickness, as well as RV hypertrophy. Interestingly, while LPA1$^{-/-}$2$^{-/-}$ mice showed exacerbated responses to hypoxia, we noted certain histological differences in lungs and hearts between these mice and WT controls at

baseline (normoxia). In normoxic WT mice, most of the small arterioles were non-muscularized in the lung. However, more than half of the small arterioles in $LPA1^{-/-}2^{-/-}$ mice were muscularized (63% versus 18% of WT mice). The average thickness of pulmonary arteriolar wall was also significantly greater in normoxic $LPA1^{-/-}2^{-/-}$ mice (6.0 $\pm$ 0.4 μm versus 4.6 $\pm$ 0.3 μm of WT, $p<0.05$). Both data indicated more remodeling in the pulmonary vasculature of $LPA1^{-/-}2^{-/-}$ mice at baseline. In the heart, the RV to heart cross-section diameter ratio was also higher in $LPA1^{-/-}2^{-/-}$ mice (0.16 $\pm$ 0.05 versus 0.11 $\pm$ 0.02 of WT), suggesting RV hypertrophy of $LPA1^{-/-}2^{-/-}$ mice at baseline. Taken together, these data again suggest that mice lacking LPA1 and LPA2 receptors may develop pulmonary hypertension without hypoxia stimulation.

In conclusion, our data provide novel evidences for LPA's regulatory role in the pulmonary vasculature. By studying mouse models with elevated and reduced LPA levels, as well as impaired LPA signaling, our data suggest that signaling through LPA1 and 2 are necessary for pulmonary development as well as the maintenance of normal pulmonary vascular pressure.

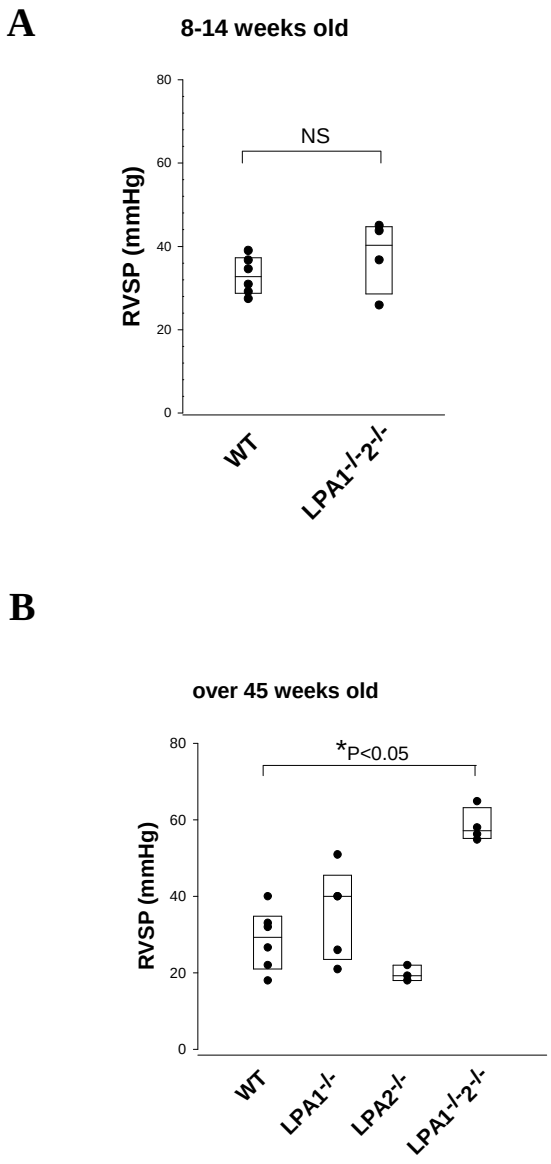

Figure 4.1. Elevation of right ventricular systolic pressures (RVSP) and RV hypertrophy of aged $LPA1^{-/-}2^{-/-}$ mice.

A. RVSP OF 8-14 weeks old WT (N=6) and $LPA1^{-/-}2^{-/-}$ (N=4) mice.

B. RVSP of over 45 weeks old WT (N=6), $LPA1^{-/-}$ (N=5), $LPA2^{-/-}$ (N=3), and $LPA1^{-/-}2^{-/-}$ (N=4) mice.

Individual values (dots) and medium with 25 and 75 confidence intervals (box plots) are presented. Data were analyzed by 2-way ANOVA. *P<0.05. NS: not statistically significant.

Genotype	Age (months)	N	PV velocity
WT	2-3	22	**737.17 ± 75.62**
WT	6-9	11	**712.43 ± 99.62**
LPA1$^{-/-}$2$^{-/-}$	2-3	18	**666.92 ± 151.84**
LPA1$^{-/-}$2$^{-/-}$	6-9	14	**583.66 ± 48.12**

Results are presented as mean ± SD in mm/sec.

Table 4.1. Peak flow velocity across the pulmonary valve of different age groups of LPA1$^{-/-}$2$^{-/-}$ mice.

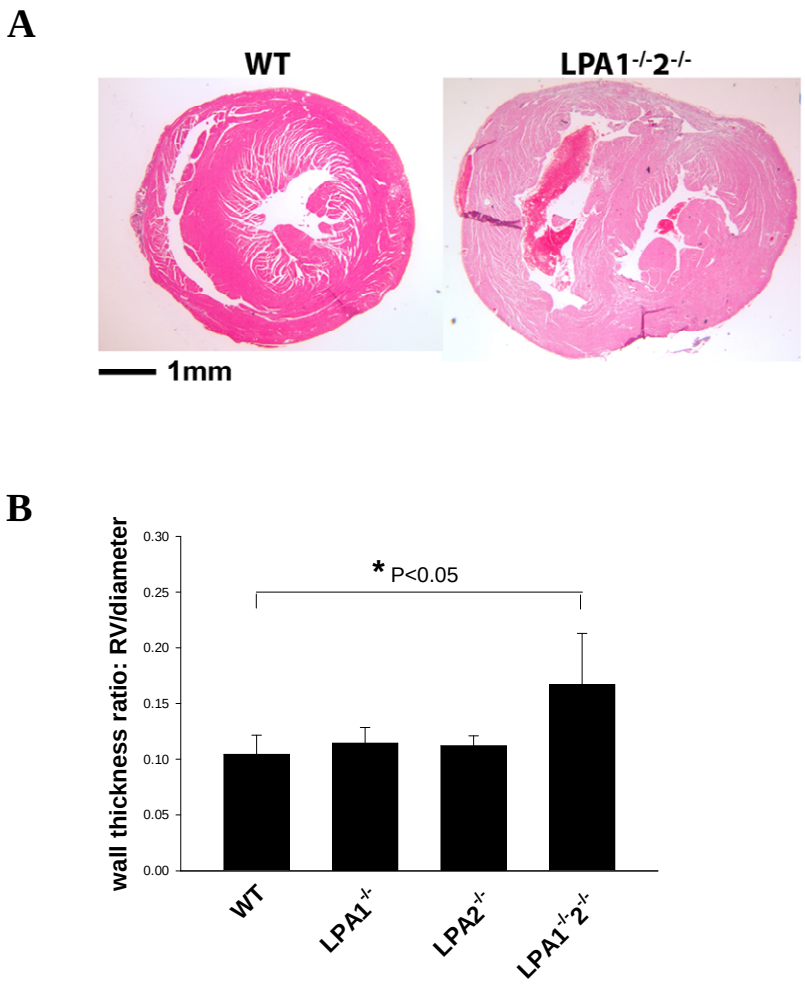

Figure 4.2. Thickening of right ventricular free wall of LPA1$^{-/-}$2$^{-/-}$ mice over 45 weeks old.

A. Representative pictures of heart cross-sections of age-matched WT and LPA1$^{-/-}$2$^{-/-}$ mice. Hearts were sectioned at the widest point transversely, and stained with H&E staining.

B. Quantification of RV free wall thickness to cross-section diameter ratio of aged mice. N=6 for WT, N=4 for LPA1$^{-/-}$, N=2 for LPA2$^{-/-}$, and N=6 for LPA1$^{-/-}$2$^{-/-}$ mice. *P<0.05.

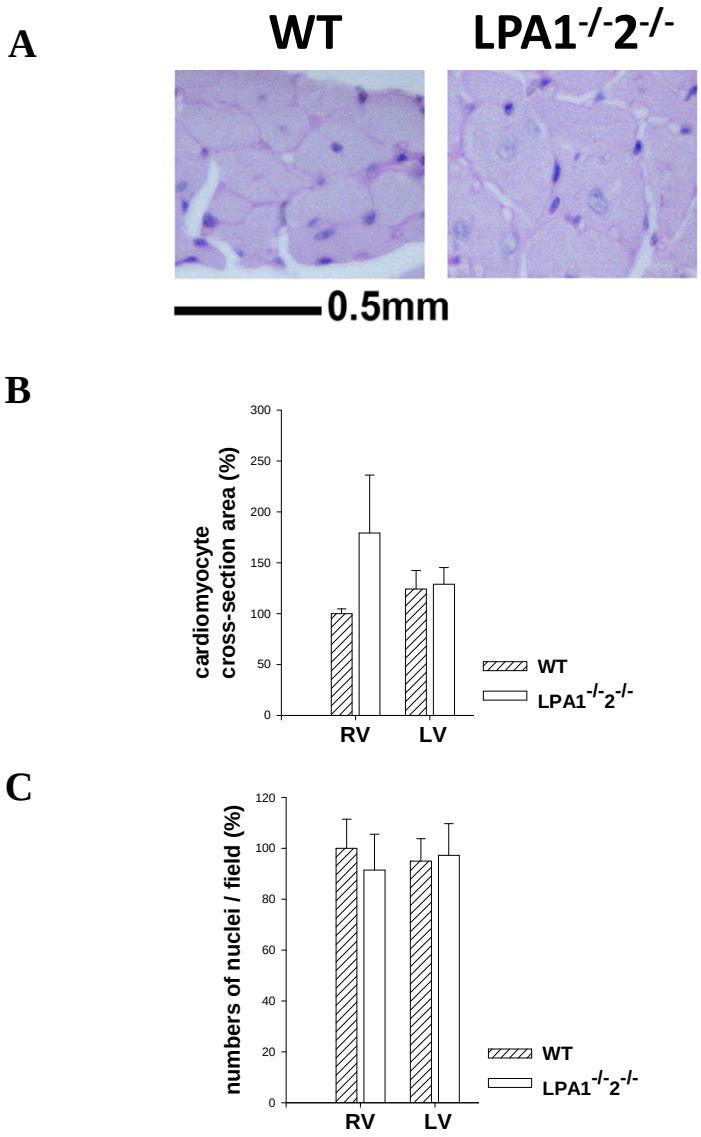

Figure 4.3. Cardiomyocyte hypertrophy of aged LPA1$^{-/-}$2$^{-/-}$ mice.

A. Representative pictures of RV cardiomyocytes of age-matched WT and LPA1$^{-/-}$2$^{-/-}$ mice. Hearts were sectioned at the widest point transversely, and stained with PAS staining.

B. Quantification of cross-section area of individual cardiomyocytes in RV and LV walls of age-matched WT (N=3) and LPA1$^{-/-}$2$^{-/-}$ (N=4) mice.

C. Average numbers of cardiomyocyte nuclear numbers in each microscopic field in RV and LV walls of age-matched WT (N=3) and LPA1$^{-/-}$2$^{-/-}$ (N=4) mice.

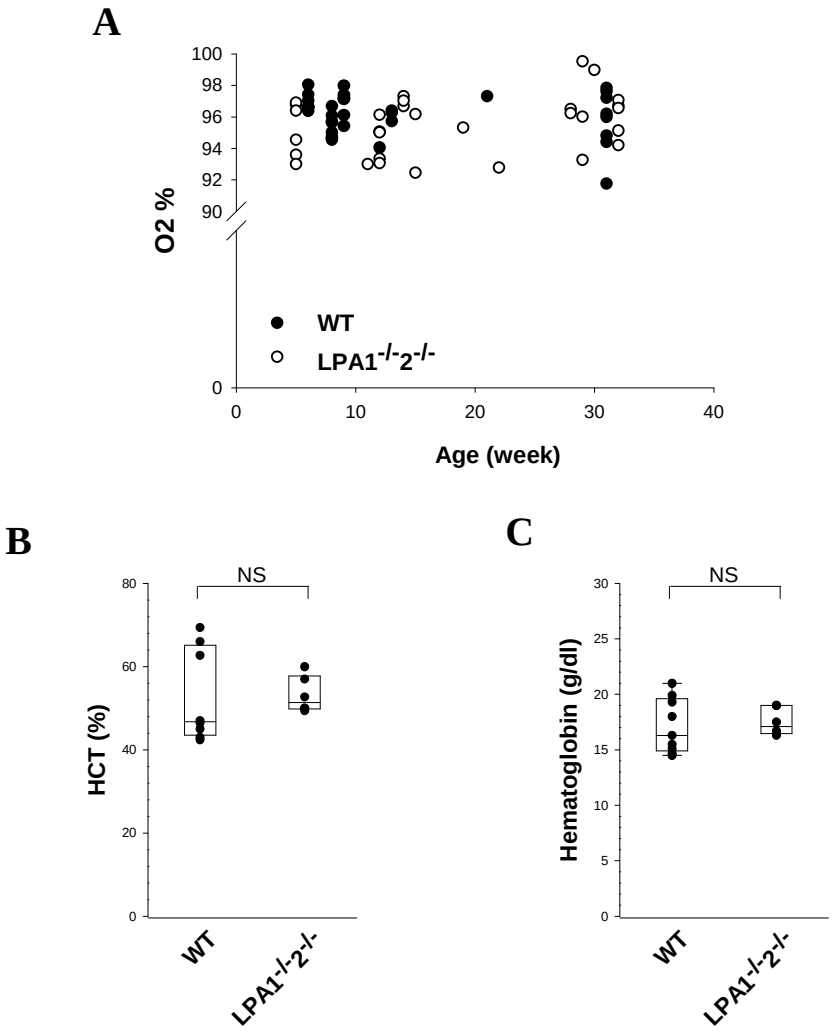

Figure 4.4. Normal arterial oxygen saturation, hematocrit , oxygen saturation and pulmonary valves of $LPA1^{-/-}2^{-/-}$ mice.

A. Arterial oxygen saturation percentage (O_2 %) of WT (closed circle) and $LPA1^{-/-}2^{-/-}$ (open circle) mice from 8 to 32 weeks old.

B. Hematocrit (HCT %) of age-matched WT (n=8) and $LPA1^{-/-}2^{-/-}$ (n=6) mice. Data are presented as individual data and box plot. Individual values (dots) and medium with 25 and 75 confidence intervals (box plots) are presented. Data were analyzed by 2-way ANOVA. NS: not statistically significant.

C. Hemaglobin concentration of age-matched WT (n=9) and $LPA1^{-/-}2^{-/-}$ (n=6) mice. Data are presented as individual data and box plot. Individual values (dots) and medium with 25 and 75 confidence intervals (box plots) are presented. Data were analyzed by 2-way ANOVA. NS: not statistically significant.

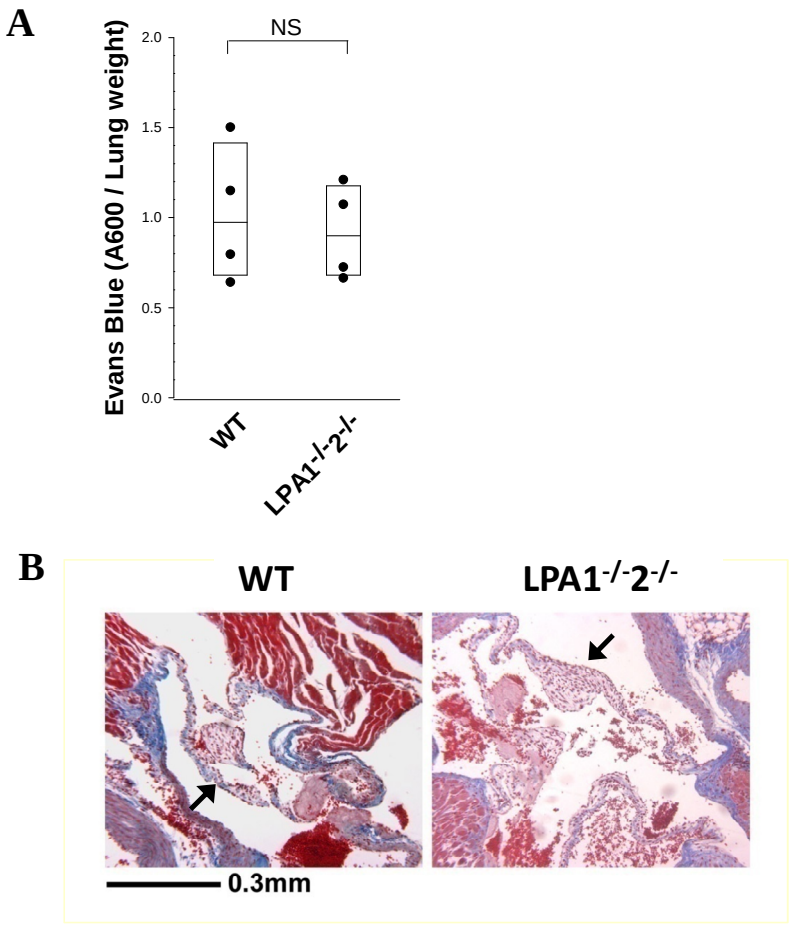

Figure 4.5. Normal pulmonary vascular permeability and pulmonary valve of LPA1$^{-/-}$2$^{-/-}$ mice.

A. Evans blue extracted from lung of age-matched WT (n=4) and LPA1$^{-/-}$2$^{-/-}$ (n=4) mice. . Data are presented as individual data and box plot. Individual values (dots) and medium with 25 and 75 confidence intervals (box plots) are presented. Data were analyzed by 2-way ANOVA. NS: not statistically significant.

B. Representative pictures of heart sections at the level of pulmonary valves of WT and LPA1$^{-/-}$2$^{-/-}$ mice. Sections were stained with Masson's trichrome staining. Pulmonary valves are indicated by arrows.

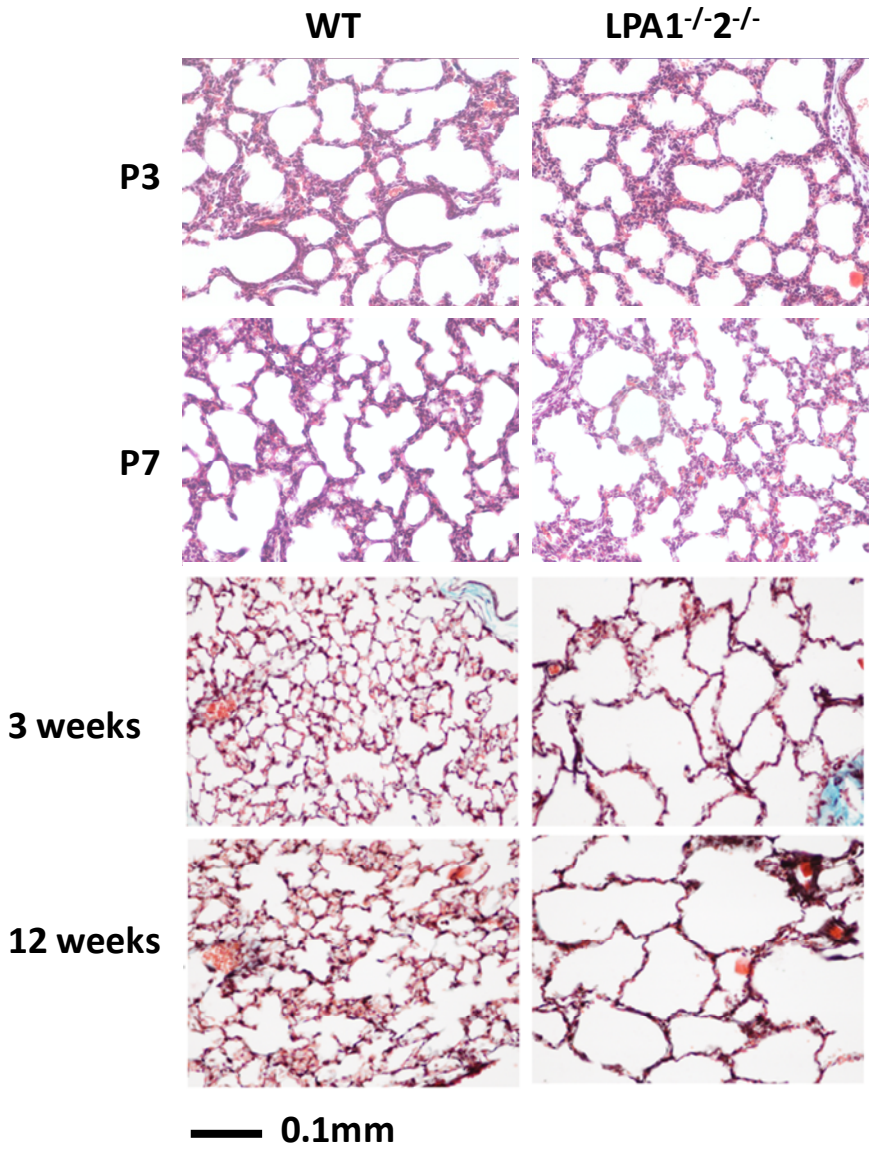

Figure 4.6. Lung histology of WT and LPA1$^{-/-}$2$^{-/-}$ mice.
Lung histology of WT and LPA1$^{-/-}$2$^{-/-}$ mice at different ages. From top to bottom: postnatal day 3 (P3), postnatal day 7 (P7), 3 weeks old, and 12 weeks old, For 3 and 12 weeks old groups, lungs were perfused by 4% paraformaldehyde through trachea, sectioned and stained with Masson's trichrome staining. For P3 and P7 groups, lungs were fixed, sectioned, and stained without perfusion. Magnification: 200x.

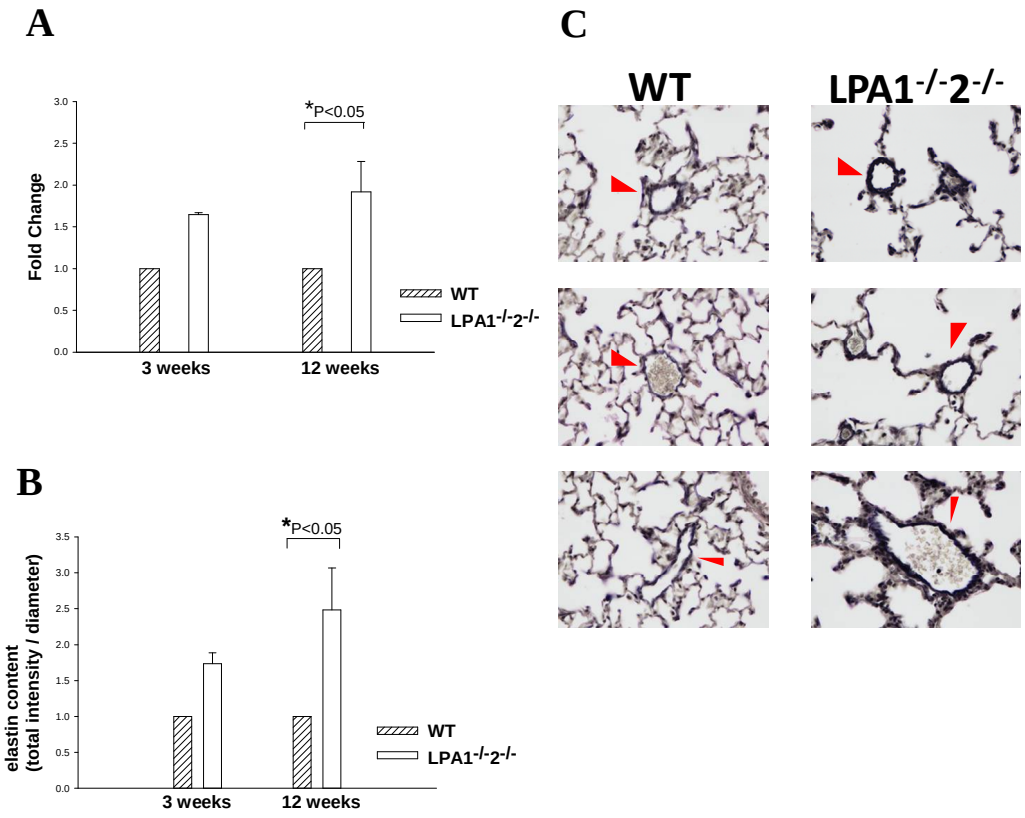

Figure 4.7. Increased perivascular elastin deposition in the lung of LPA1$^{-/-}$2$^{-/-}$ mice.

A. Quantitative RT-PCR analysis showing higher elastin expression level in lung of age-matched LPA1$^{-/-}$2$^{-/-}$ mice comparing to age-matched WT mice. N=2 for 3 weeks old group, and N=3 for 12 weeks old group. All results were presented as mean ± S.D. The expression level of WT is set as 1. *P<0.05.

B. Quantification showing higher perivascular elastin content of LPA1$^{-/-}$2$^{-/-}$ mice comparing to age-matched WT mice. n=2 for 3 weeks old group, and N=4 for 12 weeks old group. *P<0.05.

C. Representative pictures of lung sections of 12 weeks old WT and LPA1$^{-/-}$2$^{-/-}$ mice. Sections were stained with elastin staining. Vessels are indicated by arrowheads.

	N	Before	After
WT	6	633.99 ± 90.22	551.97 ± 154.02
LPA1$^{-/-}$2$^{-/-}$	5	607.66 ± 90.78	465.6 ± 149.21

Results are presented as mean ± SD. In mm/sec

Table 4.2. Peak flow velocity across the pulmonary valve before and after 3 weeks of exposure to normoxia and hypoxia.

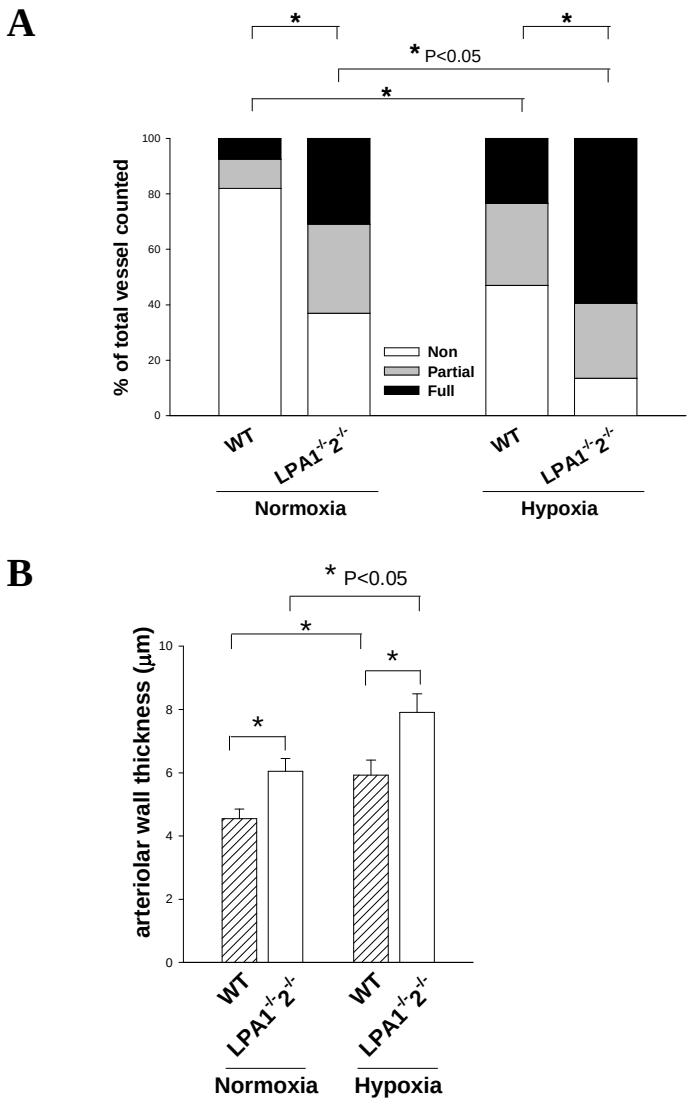

Figure 4.8. The response of mice deficient of LPA1 and 2 to hypoxia.

A. Percentages of muscularization of distal pulmonary arterioles in normoxic or hypoxic WT and LPA1$^{-/-}$2$^{-/-}$ mice. Lung sections were immunostained with a-smooth muscle actin and scored as described in Materials and Methods. non= non muscularized vessels, partial= partially muscularized vessels, and full= fully muscularized vessels. Increased numbers of fully muscularized pulmonary arterioles and less non-muscularized arterioles of LPA1$^{-/-}$2$^{-/-}$ mice, comparing to age-matched WT, are shown. Data are presented as mean ± S.D from 4 mice/group and were analyzed by 2-way ANOVA. *P<0.05.

B. Thicker pulmonary arteriolar wall of LPA1$^{-/-}$2$^{-/-}$ mice under both normoxic and hypoxic conditions, comparing to age-matched WT. N=4 mice in each group, and data are presented as mean ± S.D. *P<0.05.

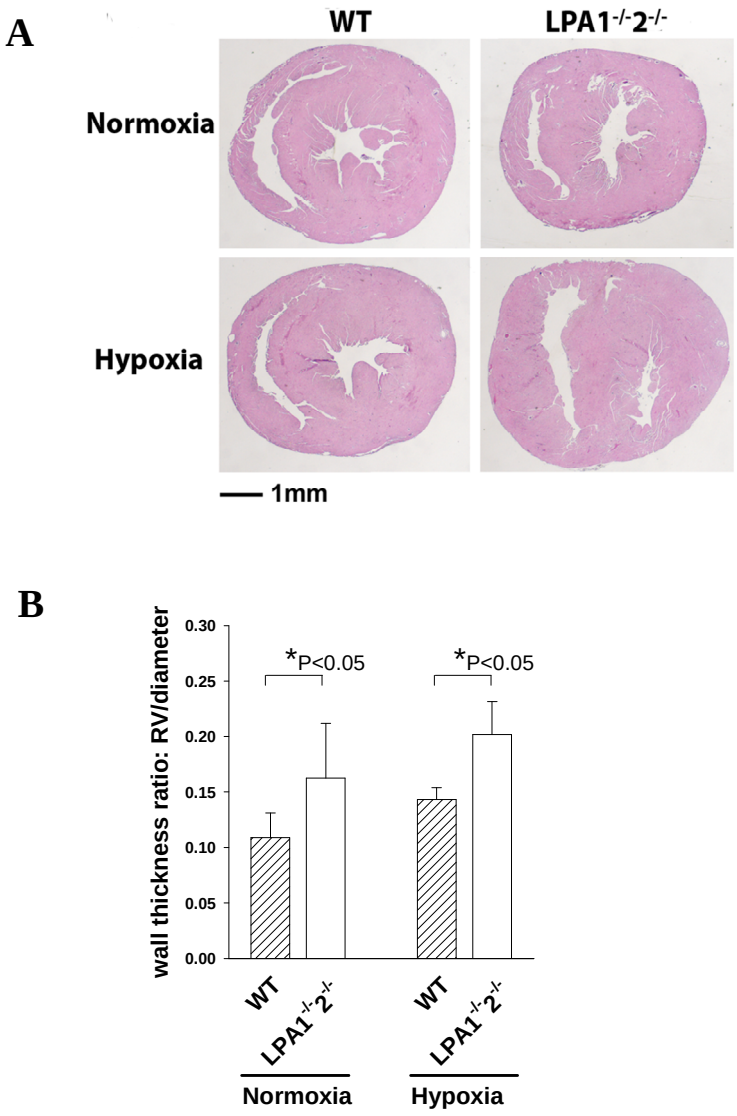

Figure 4.9. Right ventricular hypertrophy of LPA1$^{-/-}$2$^{-/-}$ mice with 21 days of hypoxia.

A. Representative pictures of cross-sections of hearts of age-matched WT and LPA1$^{-/-}$2$^{-/-}$ mice. Hearts were sectioned at the widest point transversely, and stained with H&E staining.

B. Quantification showing higher RV free wall thickness to cross-section diameter ratio of LPA1$^{-/-}$ 2$^{-/-}$ mice comparing to age-matched WT controls in both normoxic and hypoxic conditions. N=5 in each group.

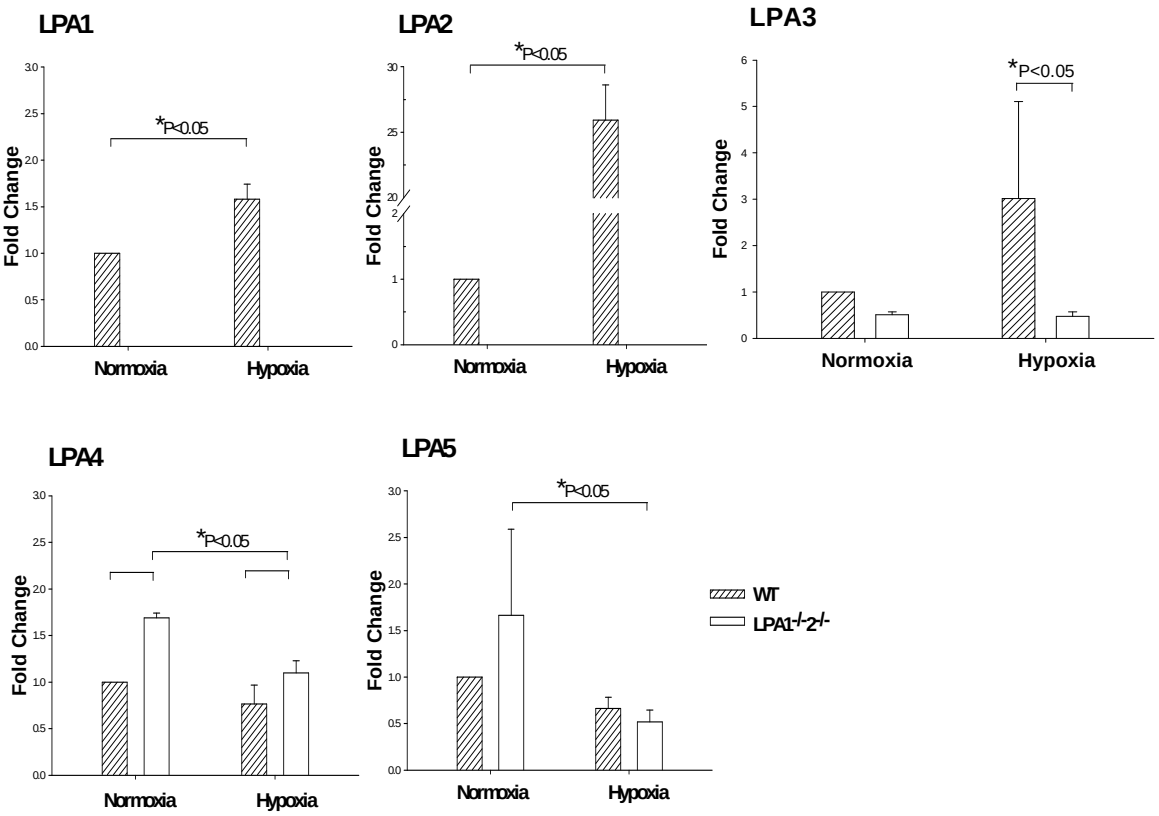

Figure 4.10. LPA receptors expression level in lung of $LPA1^{-/-}2^{-/-}$ mice. Quantitative RT-PCR analysis of LPA1-5 expression level in lung of age-matched WT (slashed bars) and $LPA1^{-/-}2^{-/-}$ (open bars) mice in normoxic and hypoxic conditions. All results were graphed from three experiments and presented as mean ± S.D. The expression level of WT mice in normoxic condition is set as 1. *P<0.05.

Chapter 5

Conclusions and future directions

Mice with reduced and elevated LPA levels

LPA is a bioactive lipid molecule present at physiologically relevant levels in plasma and serum [126]. LPA has been shown to regulate the vasculature in various aspects. Acute administration of LPA triggers vessel constriction in rats and guinea pigs[97] LPA had been proposed to contribute to phenotypic modulations such as proliferation and migration of culture vascular SMCs and appears to modulate arterial remodeling responses in carotid arteries of rodents [100]. LPA also has effects on endothelial cell function and endothelial barrier integrity [62,73,79]. Therefore we proposed that LPA may be an important mediator in the pulmonary vasculature.

The goal of this project was to determine if LPA signaling plays a role in regulation of pulmonary vasculature, specifically, the regulation of pulmonary vascular pressure. Our first strategy to evaluate a role for LPA in the pulmonary vasculature made use of mice with altered levels of circulating LPA. Mice

heterozygous of *Enpp2*, the gene encoding the major LPA producing enzyme autotaxin/lysoPLD, with ~half of circulating LPA, and transgenic mice overexpressing human *Enpp2* with increased LPA level were used to determine their reactivity in the hypoxia-induced pulmonary hypertension. Enpp2$^{+/-}$ mice showed exaggerated responses to hypoxia with greater elevation in RVSP, reduction in peak flow velocity across the pulmonary valve, and increased remodeling of the pulmonary vasculature. These findings would be consistent with a normal role for LPA in preventing hypoxia-induced pulmonary vasoconstriction. Mice overexpressing human autotaxin/lysoPLD responded similarly to their WT controls, although they did display preserved peak flow velocity across the pulmonary valve after hypoxia, which might reflect mild protection from hypoxia. The phenotype of the Enpp2-Tg mice may be due to down-regulation of transgene expression that occurs during hypoxia, or due to the fact that physiological LPA levels are sufficient to exert the protective effect and further increases may provide no additional benefit. Together, our data suggest that the maintenance of local or circulating LPA levels may offset the pulmonary vascular changes that are elicited by hypoxia. An alternate explanation is that mice with circulating defects in LPA levels develop compensatory responses that make them more prone to hypoxia-induced changes.

Mice deficient of LPA receptors 1 and 2

Having established that LPA regulates pulmonary vascular pressure, we investigated potential receptor(s) involved. Given the high expression levels of LPA1 and LPA2 in vascular SMCs and endothelial cells, we sought to determine whether LPA1 and LPA2 participate in the regulatory effect. We found that mice lacking both LPA receptors 1 and 2 ($LPA1^{-/-}2^{-/-}$ mice) developed spontaneous pulmonary hypertension with age, as evidenced by an elevation in RVSP in the absence of pulmonary valve abnormalities, a decline in peak flow velocity across the pulmonary valve, development of RV hypertrophy, and histological evidence of pulmonary vascular remodeling. While no significant difference in RVSP was found that in young adult $LPA1^{-/-}2^{-/-}$ and WT controls, the RVSP of aged $LPA1^{-/-}2^{-/-}$ mice was significantly higher than age-matched WT mice. Aged $LPA1^{-/-}$ mice may display a slightly higher RVSP than WT controls, while $LPA2^{-/-}$ mice had normal RVSP, indicating lack of LPA1 may have partial effect on the age-dependent development of pulmonary hypertension. Nevertheless, neither $LPA1^{-/-}$ and $LPA2^{-/-}$ mice displayed the significant elevation of RVSP observed in the $LPA1^{-/-}2^{-/-}$ mice, suggesting redundant signaling pathways between these two receptors, and that lack of only one receptor is not sufficient to cause the pronounced phenotype observed in the absence of both receptors. To investigate

receptor dose-dependent effects in more detail, LPA1$^{+/-}$2$^{-/-}$ and LPA1$^{-/-}$2$^{+/-}$ mice could be evaluated to determine. It would be interesting to know whether any of these strains spontaneously develop certain degree of pulmonary hypertension as did the LPA1$^{-/-}$2$^{-/-}$ mice, or they would be rather similar to the single knockout mice.

I excluded common causes of secondary pulmonary hypertension, such as hypoxia, pulmonary valve stenosis, obstruction in the main pulmonary vasculature, and thromboembolism, as the reason of elevated pulmonary pressure in LPA1$^{-/-}$2$^{-/-}$ mice. The integrity of endothelial layers in the lung was also examined by endothelial permeability assay. No significant increase in pulmonary endothelial permeability was found in LPA1$^{-/-}$2$^{-/-}$ mice. Tager and colleagues have recently reported LPA1-deficient mice are protected from bleomycin-induced lung injury, with reduced pulmonary endothelial permeability and fibrosis after the challenge [109,123]. It would be worthwhile evaluating the pulmonary permeability and fibrosis of LPA1$^{-/-}$2$^{-/-}$ mice in the lung injury model. Interestingly, Tager *et al.* stated no significant differences in the numbers of total leukocytes, macrophages, or neutrophils in the BAL of LPA1$^{-/-}$ mice, which is similar to our observations that no sign of increase in inflammatory cells infiltration in lung tissues of LPA1$^{-/-}$2$^{-/-}$ mice.

I observed enlarged alveolar spaces in the lung of LPA1$^{-/-}$2$^{-/-}$ mice. I therefore

sought to determine whether the lung development was affected by lack of LPA 1 and 2. Alveolar enlargement occurred in LPA1$^{-/-}$2$^{-/-}$ mice as early as 3 and 12 weeks of age. No obvious differences were seen at postnatal day 3 and 7, suggesting the impairment of pulmonary development likely occurred between postnatal day 7 and 21, when alveolar septation occurs. The percentages of muscularized arterioles were greater in both 3 and 12 weeks old LPA1$^{-/-}$2$^{-/-}$ mice, comparing to age-matched WT controls, suggesting the vascular remodeling was evident as early as 3 weeks of age. The fact that pulmonary histology of LPA1$^{-/-}$ and LPA2$^{-/-}$ mice appears to be normal without alveolar enlargement again suggests the redundancy of LPA1 and LPA2 in the regulation of pulmonary vasculature (data not shown).

Alveolarization and angiogenesis tightly associate and coordinate with each other during lung development, and inhibition of angiogenesis would result in impaired alveolarization [8]. The expression levels of angiogenetic markers Tie-1, VEGF, and VEGFRII in the lung tissues were similar among genotypes and normoxia/hypoxia treatments (data not shown). However, our result could be attributed to dilution of vascular cells by other cells types, such as pneumocytes, in the lung. Therefore we could not conclude that angiogenesis is not affected in the lung of LPA1$^{-/-}$2$^{-/-}$ mice without further confirmation.

Impaired alveolarization in newborns and increased pulmonary pressure later in life are the two main problems spontaneously developed in the lung of $LPA1^{-/-}2^{-/-}$ mice. Multiple reports have linked alveolarization with pulmonary hypertension. Dexamethasone treatment on neonatal rats reduces alveolarization and pulmonary artery counts. When challenged with hypoxia, rats received dexamethasone in the neonatal period displayed significant higher RVSP and RV mass [142]. Fetal lambs undergone surgery of ductus arteriosus constriction to induce pulmonary hypertension showed reduced alveolarization and small pulmonary artery density [143]. These examples suggest mutual regulations between pulmonary pressure and development. Furthermore, the pathways regulating alveolarization and pulmonary pressure may be highly associated. Lacking LPA signaling may contribute to both impaired alveolarization and pulmonary hypertension in mice, or it could have crucial effect on one event, which with time affecting the other one.

Gene expression and perivascular levels of elastin, one of the major ECM components in the lung, were up-regulated in lungs of 3 and 12 weeks old $LPA1^{-/-}2^{-/-}$ mice. The increase of perivascular elastin in $LPA1^{-/-}2^{-/-}$ mice may reflect alterations in pulmonary arterial pressure and/or abnormal vascular development in the $LPA1^{-/-}2^{-/-}$ mice.

LPA1$^{-/-}$2$^{-/-}$ mice showed exacerbated responses to hypoxia with greater decline in peak flow velocity across the pulmonary valve, pulmonary vascular remodeling, as well as RV hypertrophy. Interestingly, we noted greater muscularization percentages and vascular wall thickness in the lung of LPA1$^{-/-}$2$^{-/-}$ mice compared to WT mice in the normoxic group. In the heart, the RV to heart cross-section diameter ratio was also greater in LPA1$^{-/-}$2$^{-/-}$ mice. Both results indicate the development of spontaneous pulmonary remodeling and RV hypertrophy in young adult LPA1$^{-/-}$2$^{-/-}$ mice at baseline. These data were in accordance with the spontaneous development of pulmonary hypertension in LPA1$^{-/-}$2$^{-/-}$ mice over time.

In conclusion, our data provide novel evidences for the regulatory role of LPA in the pulmonary vasculature. By studying mouse models with elevated and reduced LPA levels, as well as mice with deficiencies in LPA receptors, our data suggest that signaling through LPA1 and 2 are necessary for pulmonary development as well as the maintenance of normal pulmonary vascular pressure.

Although no other reports have suggested the role of LPA in regulating pulmonary pressure, multiple studies have shown the regulatory effect of LPA in other vascular beds. For example, intravenous injection of LPA elevates arterial blood pressure in rats [97] and local application causes cerebral vasoconstriction in

pigs [98]. Moreover, local infusion of LPA in the rat common carotid artery induces vascular remodeling by stimulating neointimal formation [99]. A similar response was observed in mice [77]. Interestingly, these studies all indicate that LPA acts to increase blood pressure, which contradicts with our data that LPA protects against pulmonary pressure elevation. We wonder whether the protective effect we observed was due to compensation to off-set lack of LPA signaling. However, pulmonary vasculature is unique in many aspects to vascular beds in the systemic circulation, where other studies took place in. In addition, the long-term loss of LPA signaling in our models may result in different responses, such as compensatory mechanisms *in vivo,* whereas other studies monitored short-term effects by administration of exogenous LPA. To determine the role of LPA in pulmonary vascular reactivity, we will perfuse isolated mouse lungs with LPA at a constant physiological-relevant flow rate, and measure the real-time pressure to see whether acute infusion of LPA mediates pulmonary vascular pressure change. Preliminary lung perfusion experiment with physiological-relevant concentration of LPA failed to increase pulmonary pressure under conditions where vasoactive compound did, suggesting that there may be different effects of LPA on systemic and pulmonary vasculature in mice. Additional experiments may be performed to determine if LPA can block the increase in pulmonary pressure elicited by

vasoconstrictors.

Proposed molecular mechanisms

As mentioned in chapter 1, pulmonary arterial hypertension develops as a consequence of an imbalance between vasodilators and vasoconstrictors [22,27,29]. To explore how LPA signaling maintains the pulmonary pressure, the integrity of three major vasoconstricting and vadodilatory pathways in the pulmonary vasculature, nitric oxide, endothelin, and prostacyclin, will be examined.

Nitric oxide

LPA has been shown to act as a potent activator of eNOS, the major NO producing enzyme in the pulmonary vasculature. LPA activates eNOS and increase NO production in a receptor-dependent manner in cultured endothelial cells [113,144]. In the animal model, eNOS knockout mice were hyperresponsive to hypoxia and developed exaggerated elevations in RVSP and have a higher incidence to develop RV hypertrophy [37, 38]. On the other hand, mice overexpressing eNOS are protected from hypoxia-induced pulmonary hypertension [36]. The responses of Enpp2$^{+/-}$ and Enpp2-Tg mice phenocopied eNOS$^{-/-}$ and eNOS-Tg mice in hypoxia exposure. We hypothesized that the deficiency of circulating LPA level or lack of LPA1 and 2

would result in insufficient eNOS activation in response to hypoxia-induced vasoconstriction, and hence lead to pulmonary hypertension. We measured expression levels of mediators in the NO pathways, *Vegfr2*, *Pde5a*, and *Nos3* by quantitative RT-PCR. Our preliminary data show that the expression levels of all three mediators were normal in lungs of Enpp2$^{+/-,}$ Enpp2-Tg, and LPA1$^{-/-}$2$^{-/-}$ mice. Exposure to hypoxia produced a 30 – 40% increase in *Vegfr2* and *Pde5a* expression and an approximately 50% decline in *Nos3* expression in WT mice. Similar changes occurred in Enpp2$^{+/-,}$ Enpp2-Tg, and LPA1$^{-/-}$2$^{-/-}$ mice with hypoxia. Therefore there was no difference in the expression patterns among genotypes and treatments. In addition to the expression pattern, our preliminary data showed that the content of total nitrate/nitrite, the metabolites of NO, was normal in the plasma of LPA1$^{-/-}$2$^{-/-}$ mice. However, since LPA has been shown to stimulate eNOS activation without affecting eNOS protein level [113], we will perform eNOS activity assays, such as quantification of the phosphorylated form of eNOS in western blotting to determine whether eNOS signaling is inhibited in Enpp2$^{+/-}$ and/or LPA1$^{-/-}$2$^{-/-}$ mice.

Endothelin

LPA has been reported to increase endothelin expression and production in several studies. The expression level of ET-1 (*Edn1*), and the secretion of ET-1 are

both increased in LPA treated rat aortic endothelial cells [145]. LPA also up-regulates the production of ET-1 in pig cerebral microvascular endothelial cells [146,147]. We therefore sought to examine the expression levels of major mediators in the endothelin pathway. Our preliminary data show that the expression levels of *Edn1* and vasoconstrictive the ET_A receptor (*Ednra*) were constantly greater in $LPA1^{-/-}2^{-/-}$ mice than age-matched WT controls at various ages (P7 and 3 and 12 weeks old). Hypoxia reduced gene expression of the ET_B receptor (*Ednrb*), the vasodilatory and clearing receptor, in WT mice, an effect that was exacerbated in $Enpp2^{+/-}$ and $LPA1^{-/-}2^{-/-}$ mice. A recent paper reporting endothelium-specific ET_B receptor knockout mice are susceptible to hypoxia with elevated RVSP and increase in RV mass as well as remodeled pulmonary arterioles, suggesting the requirement of ET_B in limiting the development of pulmonary hypertension in response to hypoxia [148]. Our preliminary data support the model that the vasoconstrictive endothelin pathway is up-regulated due to reduction in LPA level or deficiency of LPA1 and LPA2. To confirm that the difference in gene expression is reflected in peptide levels, ELISA assays quantifying pulmonary ET-1 will be performed.

Prostacyclin

We will also examine the gene expression of mediators in the prostacyclin

pathway, not only because prostacyclin is a potent vasodilator, but also because it inhibits the production of ET-1 [149]. In addition, LPA has been reported to promote prostacyclin secretion [150]. Quantification of the metabolites of prostacyclin in mouse urine will be performed by mass spectrometry to see whether the prostacyclin pathway is affected with increased or decreased LPA signaling.

In sum, our data provide novel evidences for LPA's regulatory role in the pulmonary vasculature. By studying mouse models with elevated and reduced LPA levels, as well as deficiency of LPA receptors, our data suggest that signaling through LPA1 and 2 are necessary for pulmonary development as well as the maintenance of normal pulmonary vascular pressure.

References

1. Shi W, Bellusci S, Warburton D. Lung development and adult lung diseases. *Chest*. 2007;132:651-6.

2. Warburton D, Gauldie J, Bellusci S, Shi W. Lung development and susceptibility to chronic obstructive pulmonary disease. *Proc Am Thorac Soc*. 2006;3:668-72.

3. Schittny JC, Mund SI, Stampanoni M. Evidence and structural mechanism for late lung alveolarization. *Am J Physiol Lung Cell Mol Physiol*. 2008;294:L246-54.

4. Chinoy MR. Lung growth and development. *Front Biosci*. 2003;8:d392-415.

5. Massaro D, Massaro GD. Dexamethasone accelerates postnatal alveolar wall thinning and alters wall composition. *Am J Physiol*. 1986;251:R218-24.

6. Schachtner SK, Wang Y, Scott Baldwin H. Qualitative and quantitative analysis of embryonic pulmonary vessel formation. *Am J Respir Cell Mol Biol*. 2000;22:157-65.

7. deMello DE, Sawyer D, Galvin N, Reid LM. Early fetal development of lung vasculature. *Am J Respir Cell Mol Biol*. 1997;16:568-81.

8. Jakkula M, Le Cras TD, Gebb S, Hirth KP, Tuder RM, Voelkel NF, Abman SH. Inhibition of angiogenesis decreases alveolarization in the developing rat lung. *Am J Physiol Lung Cell Mol Physiol*. 2000;279:L600-7.

9. Rieger-Fackeldey E, Hentschel R. Bronchopulmonary dysplasia and early prophylactic inhaled nitric oxide in preterm infants: current concepts and future research strategies in animal models. *J Perinat Med*. 2008;36:442-7.

10. Deruelle P, Balasubramaniam V, Kunig AM, Seedorf GJ, Markham NE, Abman SH. BAY 41-2272, a direct activator of soluble guanylate cyclase, reduces right ventricular hypertrophy and prevents pulmonary vascular remodeling during

chronic hypoxia in neonatal rats. *Biol Neonate*. 2006;90:135-44.

11. Kalinichenko VV, Lim L, Stolz DB, Shin B, Rausa FM, Clark J, Whitsett JA, Watkins SC, Costa RH. Defects in pulmonary vasculature and perinatal lung hemorrhage in mice heterozygous null for the Forkhead Box f1 transcription factor. *Dev Biol*. 2001;235:489-506.

12. DeLisser HM, Helmke BP, Cao G, Egan PM, Taichman D, Fehrenbach M, Zaman A, Cui Z, Mohan GS, Baldwin HS, Davies PF, Savani RC. Loss of PECAM-1 function impairs alveolarization. *J Biol Chem*. 2006;281:8724-31.

13. Goumans MJ, Liu Z, ten Dijke P. TGF-beta signaling in vascular biology and dysfunction. *Cell Res*. 2009;19:116-27.

14. Gauldie J, Galt T, Bonniaud P, Robbins C, Kelly M, Warburton D. Transfer of the active form of transforming growth factor-beta 1 gene to newborn rat lung induces changes consistent with bronchopulmonary dysplasia. *Am J Pathol*. 2003;163:2575-84.

15. Vicencio AG, Lee CG, Cho SJ, Eickelberg O, Chuu Y, Haddad GG, Elias JA. Conditional overexpression of bioactive transforming growth factor-beta1 in neonatal mouse lung: a new model for bronchopulmonary dysplasia? *Am J Respir Cell Mol Biol*. 2004;31:650-6.

16. Kulkarni AB, Ward JM, Yaswen L, Mackall CL, Bauer SR, Huh CG, Gress RE, Karlsson S. Transforming growth factor-beta 1 null mice. An animal model for inflammatory disorders. *Am J Pathol*. 1995;146:264-75.

17. Ambalavanan N, Nicola T, Hagood J, Bulger A, Serra R, Murphy-Ullrich J, Oparil S, Chen YF. Transforming growth factor-beta signaling mediates hypoxia-induced pulmonary arterial remodeling and inhibition of alveolar development in newborn mouse lung. *Am J Physiol Lung Cell Mol Physiol*. 2008;295:L86-95.

18. Nicola T, Hagood JS, James ML, Macewen MW, Williams TA, Hewitt MM, Schwiebert L, Bulger A, Oparil S, Chen YF, Ambalavanan N. Loss of Thy-1 inhibits alveolar development in the newborn mouse lung. *Am J Physiol Lung Cell Mol Physiol*. 2009;296:L738-50.

19. Bonniaud P, Kolb M, Galt T, Robertson J, Robbins C, Stampfli M, Lavery C, Margetts PJ, Roberts AB, Gauldie J. Smad3 null mice develop airspace enlargement and are resistant to TGF-beta-mediated pulmonary fibrosis. *J Immunol*. 2004;173:2099-108.

20. Chen H, Sun J, Buckley S, Chen C, Warburton D, Wang XF, Shi W. Abnormal mouse lung alveolarization caused by Smad3 deficiency is a developmental antecedent of centrilobular emphysema. *Am J Physiol Lung Cell Mol Physiol*. 2005;288:L683-91.

21. Alejandre-Alcazar MA, Michiels-Corsten M, Vicencio AG, Reiss I, Ryu J, de Krijger RR, Haddad GG, Tibboel D, Seeger W, Eickelberg O, Morty RE. TGF-beta signaling is dynamically regulated during the alveolarization of rodent and human lungs. *Dev Dyn*. 2008;237:259-69.

22. De Marco T. Pulmonary arterial hypertension and women. *Cardiol Rev*. 2006;14:312-8.

23. Rabinovitch M. Molecular pathogenesis of pulmonary arterial hypertension. *J Clin Invest*. 2008;118:2372-9.

24. Gaine S. Pulmonary hypertension. *Jama*. 2000;284:3160-8.

25. D'Alonzo GE, Barst RJ, Ayres SM, Bergofsky EH, Brundage BH, Detre KM, Fishman AP, Goldring RM, Groves BM, Kernis JT, et al. Survival in patients with primary pulmonary hypertension. Results from a national prospective registry. *Ann Intern Med*. 1991;115:343-9.

26. Humbert M, Sitbon O, Chaouat A, Bertocchi M, Habib G, Gressin V, Yaici A, Weitzenblum E, Cordier JF, Chabot F, Dromer C, Pison C, Reynaud-Gaubert M, Haloun A, Laurent M, Hachulla E, Simonneau G. Pulmonary arterial hypertension in France: results from a national registry. *Am J Respir Crit Care Med*. 2006;173:1023-30.

27. McLaughlin VV, McGoon MD. Pulmonary arterial hypertension. *Circulation*. 2006;114:1417-31.

28. Michelakis ED, Wilkins MR, Rabinovitch M. Emerging concepts and translational priorities in pulmonary arterial hypertension. *Circulation*. 2008;118:1486-95.

29. Humbert M, Sitbon O, Simonneau G. Treatment of pulmonary arterial hypertension. *N Engl J Med*. 2004;351:1425-36.

30. Farber HW. The status of pulmonary arterial hypertension in 2008. *Circulation*. 2008;117:2966-8.

31. Humbert M, Morrell NW, Archer SL, Stenmark KR, MacLean MR, Lang IM, Christman BW, Weir EK, Eickelberg O, Voelkel NF, Rabinovitch M. Cellular and molecular pathobiology of pulmonary arterial hypertension. *J Am Coll Cardiol*. 2004;43:13S-24S.

32. Shaul PW, Afshar S, Gibson LL, Sherman TS, Kerecman JD, Grubb PH, Yoder BA, McCurnin DC. Developmental changes in nitric oxide synthase isoform expression and nitric oxide production in fetal baboon lung. *Am J Physiol Lung Cell Mol Physiol*. 2002;283:L1192-9.

33. Musicki B, Burnett AL. eNOS function and dysfunction in the penis. *Exp Biol Med (Maywood)*. 2006;231:154-65.

34. Giaid A, Saleh D, Yanagisawa M, Forbes RD. Endothelin-1 immunoreactivity and mRNA in the transplanted human heart. *Transplantation*. 1995;59:1308-13.

35. Huang PL, Huang Z, Mashimo H, Bloch KD, Moskowitz MA, Bevan JA, Fishman MC. Hypertension in mice lacking the gene for endothelial nitric oxide synthase. *Nature*. 1995;377:239-42.

36. Ozaki M, Kawashima S, Yamashita T, Ohashi Y, Rikitake Y, Inoue N, Hirata KI, Hayashi Y, Itoh H, Yokoyama M. Reduced hypoxic pulmonary vascular remodeling by nitric oxide from the endothelium. *Hypertension*. 2001;37:322-7.

37. Steudel W, Scherrer-Crosbie M, Bloch KD, Weimann J, Huang PL, Jones RC, Picard MH, Zapol WM. Sustained pulmonary hypertension and right ventricular hypertrophy after chronic hypoxia in mice with congenital deficiency of nitric

oxide synthase 3. *J Clin Invest*. 1998;101:2468-77.

38. Fagan KA, Fouty BW, Tyler RC, Morris KG, Jr., Hepler LK, Sato K, LeCras TD, Abman SH, Weinberger HD, Huang PL, McMurtry IF, Rodman DM. The pulmonary circulation of homozygous or heterozygous eNOS-null mice is hyperresponsive to mild hypoxia. *J Clin Invest*. 1999;103:291-9.

39. Balasubramaniam V, Tang JR, Maxey A, Plopper CG, Abman SH. Mild hypoxia impairs alveolarization in the endothelial nitric oxide synthase-deficient mouse. *Am J Physiol Lung Cell Mol Physiol*. 2003;284:L964-71.

40. Sperling RT, Creager MA. Nitric oxide and pulmonary hypertension. *Coron Artery Dis*. 1999;10:287-94.

41. Shaul PW. Regulation of endothelial nitric oxide synthase: location, location, location. *Annu Rev Physiol*. 2002;64:749-74.

42. Arehart E, Gleim S, Kasza Z, Fetalvero KM, Martin KA, Hwa J. Prostacyclin, atherothrombosis, and cardiovascular disease. *Curr Med Chem*. 2007;14:2161-9.

43. Cheng Y, Austin SC, Rocca B, Koller BH, Coffman TM, Grosser T, Lawson JA, FitzGerald GA. Role of prostacyclin in the cardiovascular response to thromboxane A2. *Science*. 2002;296:539-41.

44. Grosser T, Fries S, FitzGerald GA. Biological basis for the cardiovascular consequences of COX-2 inhibition: therapeutic challenges and opportunities. *J Clin Invest*. 2006;116:4-15.

45. Cathcart MC, Tamosiuniene R, Chen G, Neilan TG, Bradford A, O'Byrne KJ, Fitzgerald DJ, Pidgeon GP. Cyclooxygenase-2-linked attenuation of hypoxia-induced pulmonary hypertension and intravascular thrombosis. *J Pharmacol Exp Ther*. 2008;326:51-8.

46. Hoshikawa Y, Voelkel NF, Gesell TL, Moore MD, Morris KG, Alger LA, Narumiya S, Geraci MW. Prostacyclin receptor-dependent modulation of pulmonary vascular remodeling. *Am J Respir Crit Care Med*. 2001;164:314-8.

47. Christman BW, McPherson CD, Newman JH, King GA, Bernard GR, Groves

BM, Loyd JE. An imbalance between the excretion of thromboxane and prostacyclin metabolites in pulmonary hypertension. *N Engl J Med*. 1992;327:70-5.

48. Teder P, Noble PW. A cytokine reborn? Endothelin-1 in pulmonary inflammation and fibrosis. *Am J Respir Cell Mol Biol*. 2000;23:7-10.

49. Giaid A, Michel RP, Stewart DJ, Sheppard M, Corrin B, Hamid Q. Expression of endothelin-1 in lungs of patients with cryptogenic fibrosing alveolitis. *Lancet*. 1993;341:1550-4.

50. Stewart DJ, Kubac G, Costello KB, Cernacek P. Increased plasma endothelin-1 in the early hours of acute myocardial infarction. *J Am Coll Cardiol*. 1991;18:38-43.

51. Rubens C, Ewert R, Halank M, Wensel R, Orzechowski HD, Schultheiss HP, Hoeffken G. Big endothelin-1 and endothelin-1 plasma levels are correlated with the severity of primary pulmonary hypertension. *Chest*. 2001;120:1562-9.

52. von Websky K, Heiden S, Pfab T, Hocher B. Pathophysiology of the endothelin system - lessons from genetically manipulated animal models. *Eur J Med Res*. 2009;14:1-6.

53. Zollmann FS, Paul M. Transgenic models for the study of endothelin function in the cardiovascular system. *J Cardiovasc Pharmacol*. 2000;35:S13-6.

54. Kurihara Y, Kurihara H, Suzuki H, Kodama T, Maemura K, Nagai R, Oda H, Kuwaki T, Cao WH, Kamada N, et al. Elevated blood pressure and craniofacial abnormalities in mice deficient in endothelin-1. *Nature*. 1994;368:703-10.

55. Hocher B, Schwarz A, Fagan KA, Thone-Reineke C, El-Hag K, Kusserow H, Elitok S, Bauer C, Neumayer HH, Rodman DM, Theuring F. Pulmonary fibrosis and chronic lung inflammation in ET-1 transgenic mice. *Am J Respir Cell Mol Biol*. 2000;23:19-26.

56. Hocher B, Thone-Reineke C, Rohmeiss P, Schmager F, Slowinski T, Burst V, Siegmund F, Quertermous T, Bauer C, Neumayer HH, Schleuning WD, Theuring F. Endothelin-1 transgenic mice develop glomerulosclerosis, interstitial fibrosis, and renal cysts but not hypertension. *J Clin Invest*. 1997;99:1380-9.

57. Hansmann G, de Jesus Perez VA, Alastalo TP, Alvira CM, Guignabert C, Bekker JM, Schellong S, Urashima T, Wang L, Morrell NW, Rabinovitch M. An antiproliferative BMP-2/PPARgamma/apoE axis in human and murine SMCs and its role in pulmonary hypertension. *J Clin Invest*. 2008;118:1846-57.

58. Morrell NW, Adnot S, Archer SL, Dupuis J, Jones PL, MacLean MR, McMurtry IF, Stenmark KR, Thistlethwaite PA, Weissmann N, Yuan JX, Weir EK. Cellular and molecular basis of pulmonary arterial hypertension. *J Am Coll Cardiol*. 2009;54:S20-31.

59. Humbert M, Montani D, Perros F, Dorfmuller P, Adnot S, Eddahibi S. Endothelial cell dysfunction and cross talk between endothelium and smooth muscle cells in pulmonary arterial hypertension. *Vascul Pharmacol*. 2008;49:113-8.

60. Teichert-Kuliszewska K, Kutryk MJ, Kuliszewski MA, Karoubi G, Courtman DW, Zucco L, Granton J, Stewart DJ. Bone morphogenetic protein receptor-2 signaling promotes pulmonary arterial endothelial cell survival: implications for loss-of-function mutations in the pathogenesis of pulmonary hypertension. *Circ Res*. 2006;98:209-17.

61. Morrell NW, Yang X, Upton PD, Jourdan KB, Morgan N, Sheares KK, Trembath RC. Altered growth responses of pulmonary artery smooth muscle cells from patients with primary pulmonary hypertension to transforming growth factor-beta(1) and bone morphogenetic proteins. *Circulation*. 2001;104:790-5.

62. Moolenaar WH, van Meeteren LA, Giepmans BN. The ins and outs of lysophosphatidic acid signaling. *Bioessays*. 2004;26:870-81.

63. Pamuklar Z, Federico L, Liu S, Umezu-Goto M, Dong A, Panchatcharam M, Fulerson Z, Berdyshev E, Natarajan V, Fang X, van Meeteren LA, Moolenaar WH, Mills GB, Morris AJ, Smyth SS. Autotaxin/lysopholipase D and lysophosphatidic acid regulate murine hemostasis and thrombosis. *J Biol Chem*. 2009;284:7385-94.

64. Smyth SS, Cheng HY, Miriyala S, Panchatcharam M, Morris AJ. Roles of lysophosphatidic acid in cardiovascular physiology and disease. *Biochim Biophys Acta*. 2008;1781:563-70.

65. Tanaka M, Okudaira S, Kishi Y, Ohkawa R, Iseki S, Ota M, Noji S, Yatomi Y, Aoki J, Arai H. Autotaxin stabilizes blood vessels and is required for embryonic vasculature by producing lysophosphatidic acid. *J Biol Chem*. 2006;281:25822-30.

66. van Meeteren LA, Ruurs P, Stortelers C, Bouwman P, van Rooijen MA, Pradere JP, Pettit TR, Wakelam MJ, Saulnier-Blache JS, Mummery CL, Moolenaar WH, Jonkers J. Autotaxin, a secreted lysophospholipase D, is essential for blood vessel formation during development. *Mol Cell Biol*. 2006;26:5015-22.

67. Brindley DN. Lipid phosphate phosphatases and related proteins: signaling functions in development, cell division, and cancer. *J Cell Biochem*. 2004;92:900-12.

68. Sciorra VA, Morris AJ. Roles for lipid phosphate phosphatases in regulation of cellular signaling. *Biochim Biophys Acta*. 2002;1582:45-51.

69. Sigal YJ, McDermott MI, Morris AJ. Integral membrane lipid phosphatases/phosphotransferases: common structure and diverse functions. *Biochem J*. 2005;387:281-93.

70. Zhang N, Sundberg JP, Gridley T. Mice mutant for Ppap2c, a homolog of the germ cell migration regulator wunen, are viable and fertile. *Genesis*. 2000;27:137-40.

71. Tomsig JL, Snyder AH, Berdyshev EV, Skobeleva A, Mataya C, Natarajan V, Brindley DN, Lynch KR. Lipid phosphate phosphohydrolase type 1 (LPP1) degrades extracellular lysophosphatidic acid in vivo. *Biochem J*. 2009;419:611-8.

72. Escalante-Alcalde D, Hernandez L, Le Stunff H, Maeda R, Lee HS, Jr Gang C, Sciorra VA, Daar I, Spiegel S, Morris AJ, Stewart CL. The lipid phosphatase LPP3 regulates extra-embryonic vasculogenesis and axis patterning. *Development*. 2003;130:4623-37.

73. Lee CW, Rivera R, Gardell S, Dubin AE, Chun J. GPR92 as a new G12/13- and Gq-coupled lysophosphatidic acid receptor that increases cAMP, LPA5. *J Biol Chem*. 2006;281:23589-97.

74. Brinkmann V. Sphingosine 1-phosphate receptors in health and disease:

mechanistic insights from gene deletion studies and reverse pharmacology. *Pharmacol Ther*. 2007;115:84-105.

75. Noguchi K, Herr D, Mutoh T, Chun J. Lysophosphatidic acid (LPA) and its receptors. *Curr Opin Pharmacol*. 2009;9:15-23.

76. McIntyre TM, Pontsler AV, Silva AR, St Hilaire A, Xu Y, Hinshaw JC, Zimmerman GA, Hama K, Aoki J, Arai H, Prestwich GD. Identification of an intracellular receptor for lysophosphatidic acid (LPA): LPA is a transcellular PPARgamma agonist. *Proc Natl Acad Sci U S A*. 2003;100:131-6.

77. Zhang C, Baker DL, Yasuda S, Makarova N, Balazs L, Johnson LR, Marathe GK, McIntyre TM, Xu Y, Prestwich GD, Byun HS, Bittman R, Tigyi G. Lysophosphatidic acid induces neointima formation through PPARgamma activation. *J Exp Med*. 2004;199:763-74.

78. Yang AH, Ishii I, Chun J. In vivo roles of lysophospholipid receptors revealed by gene targeting studies in mice. *Biochim Biophys Acta*. 2002;1582:197-203.

79. Ishii I, Fukushima N, Ye X, Chun J. Lysophospholipid receptors: signaling and biology. *Annu Rev Biochem*. 2004;73:321-54.

80. Fukushima N, Ishii I, Contos JJ, Weiner JA, Chun J. Lysophospholipid receptors. *Annu Rev Pharmacol Toxicol*. 2001;41:507-34.

81. Contos JJ, Fukushima N, Weiner JA, Kaushal D, Chun J. Requirement for the lpA1 lysophosphatidic acid receptor gene in normal suckling behavior. *Proc Natl Acad Sci U S A*. 2000;97:13384-9.

82. Hama K, Aoki J, Inoue A, Endo T, Amano T, Motoki R, Kanai M, Ye X, Chun J, Matsuki N, Suzuki H, Shibasaki M, Arai H. Embryo spacing and implantation timing are differentially regulated by LPA3-mediated lysophosphatidic acid signaling in mice. *Biol Reprod*. 2007;77:954-9.

83. Ye X, Hama K, Contos JJ, Anliker B, Inoue A, Skinner MK, Suzuki H, Amano T, Kennedy G, Arai H, Aoki J, Chun J. LPA3-mediated lysophosphatidic acid signalling in embryo implantation and spacing. *Nature*. 2005;435:104-8.

84. Contos JJ, Ishii I, Fukushima N, Kingsbury MA, Ye X, Kawamura S, Brown JH, Chun J. Characterization of lpa(2) (Edg4) and lpa(1)/lpa(2) (Edg2/Edg4) lysophosphatidic acid receptor knockout mice: signaling deficits without obvious phenotypic abnormality attributable to lpa(2). *Mol Cell Biol*. 2002;22:6921-9.

85. Lee Z, Cheng CT, Zhang H, Subler MA, Wu J, Mukherjee A, Windle JJ, Chen CK, Fang X. Role of LPA4/p2y9/GPR23 in negative regulation of cell motility. *Mol Biol Cell*. 2008;19:5435-45.

86. Kawai-Kowase K, Owens GK. Multiple repressor pathways contribute to phenotypic switching of vascular smooth muscle cells. *Am J Physiol Cell Physiol*. 2007;292:C59-69.

87. Owens GK. Regulation of differentiation of vascular smooth muscle cells. *Physiol Rev*. 1995;75:487-517.

88. Hayashi K, Takahashi M, Nishida W, Yoshida K, Ohkawa Y, Kitabatake A, Aoki J, Arai H, Sobue K. Phenotypic modulation of vascular smooth muscle cells induced by unsaturated lysophosphatidic acids. *Circ Res*. 2001;89:251-8.

89. Siess W, Tigyi G. Thrombogenic and atherogenic activities of lysophosphatidic acid. *J Cell Biochem*. 2004;92:1086-94.

90. Xu YJ, Aziz OA, Bhugra P, Arneja AS, Mendis MR, Dhalla NS. Potential role of lysophosphatidic acid in hypertension and atherosclerosis. *Can J Cardiol*. 2003;19:1525-36.

91. Gennero I, Xuereb JM, Simon MF, Girolami JP, Bascands JL, Chap H, Boneu B, Sie P. Effects of lysophosphatidic acid on proliferation and cytosolic Ca++ of human adult vascular smooth muscle cells in culture. *Thromb Res*. 1999;94:317-26.

92. Boguslawski G, Grogg JR, Welch Z, Ciechanowicz S, Sliva D, Kovala AT, McGlynn P, Brindley DN, Rhoades RA, English D. Migration of vascular smooth muscle cells induced by sphingosine 1-phosphate and related lipids: potential role in the angiogenic response. *Exp Cell Res*. 2002;274:264-74.

93. Damirin A, Tomura H, Komachi M, Liu JP, Mogi C, Tobo M, Wang JQ,

Kimura T, Kuwabara A, Yamazaki Y, Ohta H, Im DS, Sato K, Okajima F. Role of lipoprotein-associated lysophospholipids in migratory activity of coronary artery smooth muscle cells. *Am J Physiol Heart Circ Physiol*. 2007;292:H2513-22.

94. Cui MZ, Laag E, Sun L, Tan M, Zhao G, Xu X. Lysophosphatidic acid induces early growth response gene 1 expression in vascular smooth muscle cells: CRE and SRE mediate the transcription. *Arterioscler Thromb Vasc Biol*. 2006;26:1029-35.

95. Cui MZ, Zhao G, Winokur AL, Laag E, Bydash JR, Penn MS, Chisolm GM, Xu X. Lysophosphatidic acid induction of tissue factor expression in aortic smooth muscle cells. *Arterioscler Thromb Vasc Biol*. 2003;23:224-30.

96. Day SM, Reeve JL, Pedersen B, Farris DM, Myers DD, Im M, Wakefield TW, Mackman N, Fay WP. Macrovascular thrombosis is driven by tissue factor derived primarily from the blood vessel wall. *Blood*. 2005;105:192-8.

97. Tokumura A, Fukuzawa K, Tsukatani H. Effects of synthetic and natural lysophosphatidic acids on the arterial blood pressure of different animal species. *Lipids*. 1978;13:572-4.

98. Tigyi G, Hong L, Yakubu M, Parfenova H, Shibata M, Leffler CW. Lysophosphatidic acid alters cerebrovascular reactivity in piglets. *Am J Physiol*. 1995;268:H2048-55.

99. Yoshida K, Nishida W, Hayashi K, Ohkawa Y, Ogawa A, Aoki J, Arai H, Sobue K. Vascular remodeling induced by naturally occurring unsaturated lysophosphatidic acid in vivo. *Circulation*. 2003;108:1746-52.

100. Panchatcharam M, Miriyala S, Yang F, Rojas M, End C, Vallant C, Dong A, Lynch K, Chun J, Morris AJ, Smyth SS. Lysophosphatidic acid receptors 1 and 2 play roles in regulation of vascular injury responses but not blood pressure. *Circ Res*. 2008;103:662-70.

101. Avraamides C, Bromberg ME, Gaughan JP, Thomas SM, Tsygankov AY, Panetti TS. Hic-5 promotes endothelial cell migration to lysophosphatidic acid. *Am J Physiol Heart Circ Physiol*. 2007;293:H193-203.

102. Panetti TS, Nowlen J, Mosher DF. Sphingosine-1-phosphate and lysophosphatidic acid stimulate endothelial cell migration. *Arterioscler Thromb Vasc Biol*. 2000;20:1013-9.

103. Panetti TS. Differential effects of sphingosine 1-phosphate and lysophosphatidic acid on endothelial cells. *Biochim Biophys Acta*. 2002;1582:190-6.

104. English D, Kovala AT, Welch Z, Harvey KA, Siddiqui RA, Brindley DN, Garcia JG. Induction of endothelial cell chemotaxis by sphingosine 1-phosphate and stabilization of endothelial monolayer barrier function by lysophosphatidic acid, potential mediators of hematopoietic angiogenesis. *J Hematother Stem Cell Res*. 1999;8:627-34.

105. Alexander JS, Patton WF, Christman BW, Cuiper LL, Haselton FR. Platelet-derived lysophosphatidic acid decreases endothelial permeability in vitro. *Am J Physiol*. 1998;274:H115-22.

106. Minnear FL, Patil S, Bell D, Gainor JP, Morton CA. Platelet lipid(s) bound to albumin increases endothelial electrical resistance: mimicked by LPA. *Am J Physiol Lung Cell Mol Physiol*. 2001;281:L1337-44.

107. Neidlinger NA, Larkin SK, Bhagat A, Victorino GP, Kuypers FA. Hydrolysis of phosphatidylserine-exposing red blood cells by secretory phospholipase A2 generates lysophosphatidic acid and results in vascular dysfunction. *J Biol Chem*. 2006;281:775-81.

108. van Nieuw Amerongen GP, Vermeer MA, van Hinsbergh VW. Role of RhoA and Rho kinase in lysophosphatidic acid-induced endothelial barrier dysfunction. *Arterioscler Thromb Vasc Biol*. 2000;20:E127-33.

109. Tager AM, LaCamera P, Shea BS, Campanella GS, Selman M, Zhao Z, Polosukhin V, Wain J, Karimi-Shah BA, Kim ND, Hart WK, Pardo A, Blackwell TS, Xu Y, Chun J, Luster AD. The lysophosphatidic acid receptor LPA1 links pulmonary fibrosis to lung injury by mediating fibroblast recruitment and vascular leak. *Nat Med*. 2008;14:45-54.

110. Lin CI, Chen CN, Chen JH, Lee H. Lysophospholipids increase IL-8 and

MCP-1 expressions in human umbilical cord vein endothelial cells through an IL-1-dependent mechanism. *J Cell Biochem*. 2006;99:1216-32.

111. Rizza C, Leitinger N, Yue J, Fischer DJ, Wang DA, Shih PT, Lee H, Tigyi G, Berliner JA. Lysophosphatidic acid as a regulator of endothelial/leukocyte interaction. *Lab Invest*. 1999;79:1227-35.

112. Lin CI, Chen CN, Lin PW, Chang KJ, Hsieh FJ, Lee H. Lysophosphatidic acid regulates inflammation-related genes in human endothelial cells through LPA1 and LPA3. *Biochem Biophys Res Commun*. 2007;363:1001-8.

113. Kou R, Igarashi J, Michel T. Lysophosphatidic acid and receptor-mediated activation of endothelial nitric-oxide synthase. *Biochemistry*. 2002;41:4982-8.

114. James AL, Pare PD, Hogg JC. The mechanics of airway narrowing in asthma. *Am Rev Respir Dis*. 1989;139:242-6.

115. Hirshman CA, Emala CW. Actin reorganization in airway smooth muscle cells involves Gq and Gi-2 activation of Rho. *Am J Physiol*. 1999;277:L653-61.

116. Hashimoto T, Nakano Y, Yamashita M, Fang YI, Ohata H, Momose K. Role of Rho-associated protein kinase and histamine in lysophosphatidic acid-induced airway hyperresponsiveness in guinea pigs. *Jpn J Pharmacol*. 2002;88:256-61.

117. Panettieri RA, Murray RK, DePalo LR, Yadvish PA, Kotlikoff MI. A human airway smooth muscle cell line that retains physiological responsiveness. *Am J Physiol*. 1989;256:C329-35.

118. Ediger TL, Toews ML. Dual effects of lysophosphatidic acid on human airway smooth muscle cell proliferation and survival. *Biochim Biophys Acta*. 2001;1531:59-67.

119. He D, Su Y, Usatyuk PV, Spannhake EW, Kogut P, Solway J, Natarajan V, Zhao Y. Lysophosphatidic Acid Enhances Pulmonary Epithelial Barrier Integrity and Protects Endotoxin-Induced Epithelial Barrier Disruption and Lung Injury. *J Biol Chem*. 2009.

120. He D, Natarajan V, Stern R, Gorshkova IA, Solway J, Spannhake EW, Zhao Y.

Lysophosphatidic acid-induced transactivation of epidermal growth factor receptor regulates cyclo-oxygenase-2 expression and prostaglandin E(2) release via C/EBPbeta in human bronchial epithelial cells. *Biochem J*. 2008;412:153-62.

121. Barekzi E, Roman J, Hise K, Georas S, Steinke JW. Lysophosphatidic acid stimulates inflammatory cascade in airway epithelial cells. *Prostaglandins Leukot Essent Fatty Acids*. 2006;74:357-63.

122. Medoff BD, Landry AL, Wittbold KA, Sandall BP, Derby MC, Cao Z, Adams JC, Xavier RJ. CARMA3 mediates lysophosphatidic acid-stimulated cytokine secretion by bronchial epithelial cells. *Am J Respir Cell Mol Biol*. 2009;40:286-94.

123. Ley K, Zarbock A. From lung injury to fibrosis. *Nat Med*. 2008;14:20-1.

124. Ferlinz J. Right ventricular diastolic performance: compliance characteristics with focus on pulmonary hypertension, right ventricular hypertrophy, and calcium channel blockade. *Cathet Cardiovasc Diagn*. 1998;43:206-43.

125. Watanabe S. Pathophysiology of hypoxaemic pulmonary vascular diseases. *Bull Eur Physiopathol Respir*. 1987;23 Suppl 11:207s-209s.

126. Moolenaar WH. Lysophosphatidic acid, a multifunctional phospholipid messenger. *J Biol Chem*. 1995;270:12949-52.

127. Choi JW, Lee CW, Chun J. Biological roles of lysophospholipid receptors revealed by genetic null mice: an update. *Biochim Biophys Acta*. 2008;1781:531-9.

128. Lee H, Goetzl EJ, An S. Lysophosphatidic acid and sphingosine 1-phosphate stimulate endothelial cell wound healing. *Am J Physiol Cell Physiol*. 2000;278:C612-8.

129. Kim J, Keys JR, Eckhart AD. Vascular smooth muscle migration and proliferation in response to lysophosphatidic acid (LPA) is mediated by LPA receptors coupling to Gq. *Cell Signal*. 2006;18:1695-701.

130. Zhang X, Azhar G, Furr MC, Zhong Y, Wei JY. Model of functional cardiac aging: young adult mice with mild overexpression of serum response factor. *Am J*

Physiol Regul Integr Comp Physiol. 2003;285:R552-60.

131. Fox PR, Maron BJ, Basso C, Liu SK, Thiene G. Spontaneously occurring arrhythmogenic right ventricular cardiomyopathy in the domestic cat: A new animal model similar to the human disease. *Circulation*. 2000;102:1863-70.

132. Barrick CJ, Rojas M, Schoonhoven R, Smyth SS, Threadgill DW. Cardiac response to pressure overload in 129S1/SvImJ and C57BL/6J mice: temporal- and background-dependent development of concentric left ventricular hypertrophy. *Am J Physiol Heart Circ Physiol*. 2007;292:H2119-30.

133. Hu J, Verkman AS. Increased migration and metastatic potential of tumor cells expressing aquaporin water channels. *Faseb J*. 2006;20:1892-4.

134. Faber JE, Szymeczek CL, Cotecchia S, Thomas SA, Tanoue A, Tsujimoto G, Zhang H. Alpha1-adrenoceptor-dependent vascular hypertrophy and remodeling in murine hypoxic pulmonary hypertension. *Am J Physiol Heart Circ Physiol*. 2007;292:H2316-23.

135. Irwin DC, Patot MT, Tucker A, Bowen R. Neutral endopeptidase null mice are less susceptible to high altitude-induced pulmonary vascular leak. *High Alt Med Biol*. 2005;6:311-9.

136. Zee ED, Schomberg S, Carpenter TC. Hypoxia upregulates lung microvascular neurokinin-1 receptor expression. *Am J Physiol Lung Cell Mol Physiol*. 2006;291:L102-10.

137. Arribas SM, Hinek A, Gonzalez MC. Elastic fibres and vascular structure in hypertension. *Pharmacol Ther*. 2006;111:771-91.

138. Wendel DP, Taylor DG, Albertine KH, Keating MT, Li DY. Impaired distal airway development in mice lacking elastin. *Am J Respir Cell Mol Biol*. 2000;23:320-6.

139. Keeley FW, Alatawi A. Response of aortic elastin synthesis and accumulation to developing hypertension and the inhibitory effect of colchicine on this response. *Lab Invest*. 1991;64:499-507.

140. Baccarani Contri M, Taparelli F, Miselli M, Bacchelli B, Biagini G. Histomorphometric, biochemical and ultrastructural changes in the aorta of salt-loaded stroke-prone spontaneously hypertensive rats fed a Japanese-style diet. *Nutr Metab Cardiovasc Dis*. 2003;13:37-45.

141. Briones AM, Gonzalez JM, Somoza B, Giraldo J, Daly CJ, Vila E, Gonzalez MC, McGrath JC, Arribas SM. Role of elastin in spontaneously hypertensive rat small mesenteric artery remodelling. *J Physiol*. 2003;552:185-95.

142. le Cras TD, Markham NE, Morris KG, Ahrens CR, McMurtry IF, Abman SH. Neonatal dexamethasone treatment increases the risk for pulmonary hypertension in adult rats. *Am J Physiol Lung Cell Mol Physiol*. 2000;278:L822-9.

143. Grover TR, Parker TA, Balasubramaniam V, Markham NE, Abman SH. Pulmonary hypertension impairs alveolarization and reduces lung growth in the ovine fetus. *Am J Physiol Lung Cell Mol Physiol*. 2005;288:L648-54.

144. Chen H, Montagnani M, Funahashi T, Shimomura I, Quon MJ. Adiponectin stimulates production of nitric oxide in vascular endothelial cells. *J Biol Chem*. 2003;278:45021-6.

145. Chua CC, Hamdy RC, Chua BH. Upregulation of endothelin-1 production by lysophosphatidic acid in rat aortic endothelial cells. *Biochim Biophys Acta*. 1998;1405:29-34.

146. Yakubu MA, Leffler CW. Regulation of ET-1 biosynthesis in cerebral microvascular endothelial cells by vasoactive agents and PKC. *Am J Physiol*. 1999;276:C300-5.

147. Yakubu MA, Leffler CW. L-type voltage-dependent Ca2+ channels in cerebral microvascular endothelial cells and ET-1 biosynthesis. *Am J Physiol Cell Physiol*. 2002;283:C1687-95.

148. Kelland NF, Bagnall AJ, Morecroft I, Gulliver-Sloan FH, Dempsie Y, Nilsen M, Yanagisawa M, Maclean MR, Kotelevtsev YV, Webb DJ. Endothelial ET(B) Limits Vascular Remodelling and Development of Pulmonary Hypertension during Hypoxia. *J Vasc Res*. 2009;47:16-22.

149. Prins BA, Hu RM, Nazario B, Pedram A, Frank HJ, Weber MA, Levin ER. Prostaglandin E2 and prostacyclin inhibit the production and secretion of endothelin from cultured endothelial cells. *J Biol Chem*. 1994;269:11938-44.

150. Woclawek-Potocka I, Kondraciuk K, Skarzynski DJ. Lysophosphatidic Acid Stimulates Prostaglandin E2 Production in Cultured Stromal Endometrial Cells Through LPA1 Receptor. *Exp Biol Med (Maywood)*. 2009;234:986-93.

151. Han RN, Bramall A, Deng Y, Yanagisawa M, McInnes R, Stewart DJ. Abnormal lung alveolarization in the ET-2 deficient mouse model: possible role of ET-2 in pulmonary vasculature development. *Circulation.* 2007;116:II 210.